

**DETECTION OF CEREBROVASCULAR DISEASE IN BRAIN IMAGES USING  
CONVOLUTIONAL NEURAL NETWORK**

BY

**LEHLOHONOLO BRIDGET SETHIBELA**

DISSERTATION

Submitted in fulfilment of the requirements for the degree of

**MASTERS OF SCIENCE**

In

**COMPUTER SCIENCE**

In the

**FACULTY OF SCIENCE AND AGRICULTURE**

**(School of Mathematical and Computer Science)**

At the

**UNIVERSITY OF LIMPOPO**

**SUPERVISOR:**

**PROF SN MOKWENA**

**2022**

## **DEDICATION**

This study is dedicated to my mother, Motlatjo Sethibela, my father, Thapelo Sethibela, and my siblings, Pertunia, Itumeleng, Katlego and Mathapelo.

## **DECLARATION**

I, Lehlohonolo Bridget Sethibela, hereby declare that the dissertation entitled “DETECTION OF CEREBROVASCULAR DISEASE USING CONVOLUTIONAL NEURAL NETWORKS”, is my original work, and all sources used have been properly cited and completely recognized. I additionally declare that this work has never before been submitted for credit at any other university.

Signature: \_\_\_\_\_

Date: \_\_\_\_\_

## **ACKNOWLEDGMENTS**

First, I want to start by giving God the glory for providing me with the courage, knowledge, and direction I needed to finish my dissertation. It gives me great pleasure to thank the following people for helping to make this research study successful:

- I am really appreciative of the help, advice, and encouragement I received from my supervisor, Prof. SN Mokwena, throughout the course of my master's degree.
- Without his open mentoring, I would never have been able to finish my studies. His helpful judgment and remarks have assisted me in finishing my dissertation.
- I'd like to thank IBM and ETDP SITA for their financial support they provided for this research study.
- In closing, I want to express my gratitude to my wonderful family for their support and affection.

## **ABSTRACT**

Cerebrovascular disease is the world's second major cause of mortality and disability, and the fourth major cause of mortality and disability in South Africa. Cerebrovascular disease occurs due to issues of the brain's blood supply, either the blood supply is cut off or a blood artery within the brain bursts. Radiologists have the responsibility to detect cerebrovascular disease. We now have technology which can help them to better detect this disease. Medical imaging plays an important role in detecting diseases. This study presents implementation of a detection system using artificial intelligence model, namely, convolutional neural networks to help in detecting cerebrovascular disease from magnetic resonance imaging (MRI) scans. Brain images using MRI was obtained from kaggle public dataset. Segmentation process was applied in this study to normalise images since the images came in different sizes. The effectiveness of the concept was demonstrated using a confusion matrix. The accuracy rate was plotted using the Receiver Operating Characteristics (ROC) curve. The evaluation results show that the Convolutional Neural Network (CNN) model detect cerebrovascular disease successfully with validation accuracy rate of 90% and test accuracy rate of 80%. The training procedure could be improved by using a larger MRI dataset.

Keywords: Cerebrovascular disease, magnetic resonance imaging (MRI), Segmentation, Convolutional Neural Network (CNN), Artificial Intelligence (AI), Medical imaging

## Table of Contents

DEDICATION .....	ii
DECLARATION.....	iii
ACKNOWLEDGMENTS.....	iv
ABSTRACT .....	v
LIST OF FIGURES.....	ix
LIST OF ABBREVIATION .....	xi
CHAPTER 1: INTRODUCTION.....	1
1.1 Introduction.....	1
1.2 Problem Statement.....	1
1.3 Motivation .....	2
1.4 Aim .....	3
1.5 Objectives.....	3
1.6 Research Questions .....	3
1.7 Methodology and Analytical Procedures.....	4
1.8 Scientific Contribution .....	4
1.9 Availability of Resources and Infrastructure.....	4
1.10 Ethical Considerations .....	4
1.11 Scope and Delimitations .....	5
1.12 Summary .....	5
1.13 Overview of Dissertation.....	5
CHAPTER 2: BACKGROUND .....	6
2.1 Introduction.....	6
2.2 Cerebrovascular Disease .....	6
2.3 Medical Imaging Techniques .....	8
2.3.1 Magnetic Resonance Imaging .....	11
2.3.2. Magnetic Resonance .....	12
2.3.3 Relaxation.....	14
2.3.4. Conventional MRI Protocols (Conventional MRI).....	16

2.3.4.1T1 Weighted Image(T1WI).....	16
2.3.4.2T2 Weighted Image .....	17
2.3.4.3 Fluid Attenuated Inversion Recovery (FLAIR).....	17
2.4. Diffusion Magnetic Resonance .....	18
2.5 Dataset .....	19
2.6 Conclusion .....	19
CHAPTER 3: LITERATURE REVIEW .....	20
3.1 Introduction.....	20
3.2 Segmentation of MRI Images for Detection of Cerebrovascular Disease .....	20
3.3 Image Object Classification-Based Methods .....	22
3.3.1 Customized Feature Methods.....	23
3.3.1.1 Decision Trees.....	23
3.3.2 Methods for Deep Learning Feature .....	24
3.3.2.1 Convolutional Neural Network Layers.....	24
3.4 Semantic Object Segmentation-Based Approaches for Images .....	27
3.4.1 Architecture for Fully Convolutional Networks (FCN).....	27
3.4.2 U-net Architecture .....	27
3.5 Measurement Metrics .....	29
3.6 Related Works in Detecting Cerebrovascular Disease .....	30
3.7 summary of related works and gaps .....	31
3.8 Conclusion .....	32
CHAPTER 4: METHODOLOGY .....	33
4.1 Introduction.....	33
4.2 Dataset .....	33
4.3 Implementation Tools .....	35
4.4 Overall Workflow of the Proposed System .....	39
4.4.1 Segmentation.....	39
4.4.2 Feature Extraction .....	40
4.4.3 CNN Model .....	40
4.4.3.1 Accuracy.....	42

4.5 Conclusion .....	43
4.6 Summary .....	43
CHAPTER 5: RESULTS.....	45
5.1 Introduction .....	45
5.2 Segmentation.....	45
5.4 CNN Model .....	51
5.5 Discussion .....	58
5.6 Conclusion .....	59
5.7 Summary .....	59
CHAPTER 6: CONCLUSION .....	61
6.1 Introduction .....	61
6.2 Research Summary .....	61
6.3 Recommendations.....	62
6.4 Conclusion .....	63
REFERENCES.....	64



## LIST OF FIGURES

Figure 2.1 The outcome of applying an RF pulse when the atoms are exposed to an outside magnetic field. ....	12
Figure 2.2 The use of a radio frequency energy pulse to ignite a magnetic nucleus.....	13
Figure 2.3 T1 recovery curve in (a) and T2 delay curve in (b) .....	14
Figure 2.4 Examples of C-MRI pictures of a cerebrovascular disease include FLAIR, T1-weighted, T1-contrast, and T2-weighted images .....	17
Figure 2.5 Example of DWI of different b value.....	18
Figure 3.1: Example of maximum pooling using a 2x2 kernel and 2 stride.....	26
Figure 3.2 U-net design example with the lowest resolution of 32x32 pixels.....	29
Figure 4.1 MRI scans.....	32
Figure 4.2 Splitting of data.....	33
Figure 4.3 Distribution of image ratios.....	34
Figure 4.4 Python libraries.....	34
Figure 4.5 Diagram of the suggested system .....	37
Figure 4.6 CNN architecture.....	39
Figure 5.1 Original image.....	44
Figure 5.2 Biggest contour.....	45
Figure 5.3 Extreme points.....	46
Figure 5.4 Cropped image.....	46

Figure 5.5 Images infected by cerebrovascular disease.....	48
Figure 5.6 Images not infected by cerebrovascular disease.....	48
Figure 5.7 Building model.....	49
Figure 5.8 Output of the CNN model.....	50
Figure 5.9 Epochs.....	51
Figure 5.10 Training epoch.....	51
Figure 5.11 Accuracy model.....	52
Figure 5.12 Model loss.....	53
Figure 5.13 Confusion matrix for validation accuracy.....	54
Figure 5.14 Confusion matrix for testing accuracy.....	55

List of tables

table 4.1 Confusion Matrix.....	41
Table 3.1 Summary of related works and gaps.....	31

## **LIST OF ABBREVIATION**

SA - South Africa

WHO -World Health Organization

CT -Computerized Tomography

MRI – Magnetic Resonance Imaging

AI -Artificial Intelligence

CNN – Convolutional Neural Network

CV - Computer vision

GM – Grey Matter

WM – White Matter

CSF – Cerebrospinal fluid

IT – Imaging Techniques

PET – Position Emission Tomography

NMR – Nuclear Magnetic Resonance

RF – Radio Frequency

FI – Free Induction

TR – Repetition Time

TE – Echo Time

C-MRI – Conventional Magnetic Resonance Imaging

WI -Weighted Image

GE - Gradient Echo

GBCA – Gadolinium Based Contrast

FLAIR - Fluid Attenuated Inversion Recovery

DWI – Diffusion weighted Imaging

SVM - support vector machine

RDF - Random-decision Forest

FCN – Fully Convolutional Network

FP – False Positive

FN -False Positive

TP – True Positive

TN – True Negative

Conv2D - Convolution layer of 2 Dimensional

ROC - Receiver Operating Characteristics

TREC – Turfloop Research Ethics Committee

## **CHAPTER 1: INTRODUCTION**

### **1.1 Introduction**

The ability of Artificial Intelligence (AI) to surpass humans on certain medical image processing tasks has piqued the research community's considerable interest. Medical imaging techniques and procedures are used to take images of various human body sections with the intention of diagnosing and treating patients. Brain is the primary organ of the body; therefore, this study focuses on implementing AI model for detection of major brain disease namely, cerebrovascular disease. This chapter presents the problem statement, in this section the problem is introduced and is followed by motivation where the reasons why this study is important to be taken are given. The key major sections that will guide the researcher when implementing the cerebrovascular disease detection system are also stated, namely, aim, objectives, research questions and methodology. The scientific contribution of the study is also given.

### **1.2 Problem Statement**

Cerebrovascular disease is the world's second major cause of mortality and disability [1], and the fourth major cause of mortality and disability in South Africa [2]. The World Health Organization (WHO) says, low and middle-income countries account for 87 percent of cerebrovascular disease-related deaths and disability. WHO ranks South Africa as a low-income country [3]. Cerebrovascular disease is a disorder in which blood flow to the brain is restricted or blocked. To get an image of the brain, radiologists frequently utilize magnetic resonance imaging (MRI), computed tomography (CT) scans, and x-rays. In order to determine whether there are any irregularities that might point to the presence of cerebrovascular disease, the radiologist examines the brain image. However, they may not always accurately determine if the disease has matured or not by examining the brain image scans with human eye [4]. The interpretation of these images is difficult due to human limitations in image analysis, such as the inability to see hidden features in the brain, which may lead to false positives and negatives [5]. Mistakes caused by incorrect

interpretation of these images may result in further brain injury or, in the worst-case, patients may lose their lives as a result of the possibility of radiologist prescribing incorrect medication.

Artificial intelligence (AI) may, however, be able to help solve this challenge, as other studies have shown that AI can outperform humans on a variety of medical-image analysis tasks such as using the Cuckoo algorithm to analyse images for heart disease detection, impetigo skin disease detection using support vector machine and Alzheimer's disease detection using pixel based method [6], [7], [8]. The existing studies on cerebrovascular disease detection used binary method which uses pixels to decide if the patient has the disease or not and they also used morphological operation which uses erosion and dilation, However, both methods do not show accuracy rate and confusion matrix which may help in interpreting the images, therefore, both methods don't outperform human beings at all since they don't provide more information about the disease [8] [9]. The studies conducted on pneumonia and breast cancer used Convolutional Neural network(CNN) model for detection, the results of pneumonia was 95% and breast cancer was 92% accurate [10], [11]. This study proposes to implement Convolutional Neural Network detection model that may produce accurate results when it comes to detecting brain abnormalities which may predispose a patient to cerebrovascular disease.

### **1.3 Motivation**

Cerebrovascular disease contributes to the global burden of diseases [1]. People die and others are suffering due to errors that are sometimes produced by radiologists when interpreting the images of the brain. AI promises to improve and enhance the work of radiologist [7]. Studies such as eczema skin detection and diabetics detection employed the CNN model for detection and the results of the studies were above 90% accurate, Eczema with 96.2% and diabetics with 94.8% detection rate [12], [13].

The existing studies on cerebrovascular disease developed a logistic regression model that predict the cerebrovascular disease given basic symptoms like age, sex, hypertension etc [14]. Another study developed a robotic arm to predict the presence of cerebrovascular disease by putting the robotic arm on the patient's arm to measure high blood

pressure level since high level of high blood pressure causes blockage of arteries which leads to cerebrovascular disease, however, both methods do not scan the body to check damages on the brain leading to possible false positives and false negatives [15]. No studies have used CNN model to improve the accuracy of detecting cerebrovascular disease. CNN has the ability of obtaining significant features in image detection tasks and provides medical promising results in image analysis [10]. AI has been dubbed the fourth industrial revolution because of its disruptive and global effects in fields such as healthcare, public health, and global health [6]. AI-based approaches have the potential to enhance individual and population health as well as global health systems [16].

#### **1.4 Aim**

The aim of the study is to detect cerebrovascular disease from brain images using Convolutional Neural Network (CNN).

#### **1.5 Objectives**

The objectives of the study are to:

- I. Automate the process of brain cropping from brain images.
- II. Implement CNN to detect any abnormalities from brain images.
- III. Test the CNN model to see if it produces accurate results.

#### **1.6 Research Questions**

The research questions of the study are as follows:

- I. How will brain cropping process from brain images be automated?
- II. How will CNN model be implemented?
- III. How will CNN model be tested to see if it produces accurate results?

## **1.7 Methodology and Analytical Procedures**

Brain images using Magnetic Resonance Imaging (MRI) were obtained from Kaggle public dataset. The dataset is divided into two folders, infected and not infected images. The dataset was divided into three subfolders, namely, training, validating and testing which contained the infected and not infected images. CNN was implemented on Jupyter notebook using python computer vision in windows 10 operating system.

The process of cropping images was done by applying image processing unit, where the input images, which are MRI brain images, went through segmentation to resize the images and separate the lesion, so as to extract the relevant information from the brain image [17]. CNN was used to detect the infected region. The effectiveness of the concept was demonstrated using a confusion matrix. The accuracy rate was plotted using the Receiver Operating Characteristics (ROC) curve.

## **1.8 Scientific Contribution**

This study will contribute to the field of medical imaging by using AI models to improve the methods that are been used to detect cerebrovascular disease. This study implemented CNN model which has been used successfully in detecting diseases such as pneumonia, breast cancer and diabetics to detect cerebrovascular disease. Successful detection of cerebrovascular disease using CNN model will save many lives especially in low income countries and developed countries.

## **1.9 Availability of Resources and Infrastructure**

The University of Limpopo's Department of Computer Science provided the necessary resources and infrastructure, including software, to undertake this research.

## **1.10 Ethical Considerations**

Since the study was based on publicly accessible data, no ethical approval was needed. All the work that was used, however, was properly referenced.



### **1.11 Scope and Delimitations**

The proposed system, namely, detection of cerebrovascular disease from brain images using CNN model used publicly available dataset from Kaggle. It is required that dataset be collected from local hospitals, so that the processes of segmentation be used in fully such as removing the noise from images, pre-processing images and using many other segmentation processes since the study used thresholding method for cropping images only.

### **1.12 Summary**

In this chapter, the study proposed to implement CNN detection model that may produce accurate results when it comes to detecting brain abnormalities which may predispose a patient to cerebrovascular disease. The study was motivated by the fact that radiologists sometimes makes mistakes when interpreting the brain images and such mistakes may lead to death and disability. CNN was implemented on Jupyter notebook using python computer vision in windows 10 operating system. The effectiveness of the concept was demonstrated using a confusion matrix. The accuracy rate was plotted using the ROC curve.

### **1.13 Overview of Dissertation**

The rest of the dissertation is organised as follows:

- Chapter 2 gives background knowledge on cerebrovascular disease in general, discusses the dataset, MRI and other modalities used to capture the image of the brain.
- Chapter 3 provides the literature review.
- Chapter 4 presents a detailed description of the design and implementation of the CNN model.
- Chapter 5 presents the research findings of the study.
- Chapter 6 presents research summary and recommendations for future studies.

## **CHAPTER 2: BACKGROUND**

### **2.1 Introduction**

Artificial intelligence has attracted the research community's intense interest as a result of its ability to outperform humans on a variety of medical image analysis tasks [6]. For the aim of diagnosis and treatment in digital health, photographs of various human body parts are captured using medical imaging techniques and procedures [7], [8].

The fundamental organ of the human body is the brain, which regulates all bodily functions such as thought, memory, touch, motor skill, vision, breathing etc [2]. Numerous illnesses, including Cerebrovascular, Alzheimer's, Dementia, and Parkinson's disease have an impact on the brain. Furthermore, cerebrovascular disease may be cancerous or noncancerous development of abnormal cells in the brain [4]. Early diagnosis of cerebrovascular disease using AI models from MRI data is of utmost importance to clinical trials, as well as the medical investigations of normal and abnormal MRI imaging [8]. The segmentation of the image is one of the most crucial steps in employing medical imaging processes to detect disorders, which isolate desired features of the MRI image for further processing and implementation of AI model that will correctly detect diseases from MRI images [17]. This chapter gives background knowledge on cerebrovascular disease in general, the techniques used to detect cerebrovascular disease, discusses the dataset, MRI and other modalities used to capture the image of the brain.

### **2.2 Cerebrovascular Disease**

The human brain controls every body function, including memory, creativity, emotion, and intelligence. The skull protects the brain, which consists of the brainstem, cerebellum, and cerebrum. The spine is joined to it by the brainstem [18]. The greatest portion of the brain is the cerebrum. The two primary forms of nerve tissue that make up the cerebrum are called White matter(WM) and Grey matter(GM). Grey matter is composed of the unmyelinated cell bodies and dendrites of neurons, whereas white matter is composed of the

myelinated axons that connect the neurons [19]. The cerebrum initiates and governs movement as well as regulates temperature.

Speech, judgment, thinking and reasoning, problem-solving, emotions, and learning are all made possible by different regions of the cerebrum [19], [20]. The cerebellum is a substantial part of the hindbrain that is located near to the brainstem. The area of the brain in charge of organizing voluntary motions numerous other aspects, including posture and motor skills like balance and coordination, are also under its control. The brainstem is the structure that connects the cerebrum of the brain with the spinal cord and cerebellum. It is divided into three parts, the midbrain, pons, and medulla oblongata, in decreasing order of size. Numerous essential aspects of life, including breathing, consciousness, blood pressure, heart rate, and sleep, are controlled by it [18], [20]. The brain's centre is made up of four interconnected hollow areas known as ventricles. Throughout the central nervous system(CNS), cerebrospinal fluid(CSF) is transported and is held in the ventricles of the brain, which are a network of linked chambers [18]. The three parts of the brain that stand out and can be seen in the photos are the GM, WM, and CSF [18].

A collection of illnesses collectively referred to as cerebrovascular disease have an impact on the brain's blood arteries and blood flow. Blood flow issues can result from artery obstruction (embolism), blood vessel rupture (haemorrhage), blood clot formation(thrombosis), blood vessel constriction (stenosis), or all of these [ 22]. A blood vessel in the brain that it serves will not be able to carry enough or any blood if there is damage to it. The absence of blood makes it difficult for enough oxygen to reach the brain, and without oxygen, brain cells will begin to deteriorate [22], [23]. Damage to the brain is permanent. To lower the danger of long-term brain injury and improve survival rates, immediate assistance is essential. Cerebrovascular disease is primarily brought on by atherosclerosis [10]. This happens when cholesterol builds up as a thick, waxy plaque that can limit or obstruct blood flow in the arteries due to excessive cholesterol levels and inflammation in the brain's arteries [24]. This plaque may partially or entirely restrict blood flow to the brain, leading to a cerebrovascular disease. Cerebrovascular disease is the world's second major cause of mortality and disability [1], and the fourth major cause of mortality and

disability in South Africa [2]. According to the WHO, low- and middle-income nations account for 87 percent of cerebrovascular disease-related mortality and disability [3].

## **2.3 Medical Imaging Techniques**

Medical imaging(MI) refers to number of non-invasive technique that are used to capture various images of organs within the body [11]. This means the body does not have to be opened or cut in order to obtain the lesion. MI is used to assist radiologist to detect and for treatment of different diseases, therefore, without MI radiologist cannot be able to detect cerebrovascular diseases at its earliest stages and be able to prescribe treatment to prevent further spread to other organs. Imaging Techniques(IT) refers to various methods used to capture the images of internal organs, there are 8 common IT used in diagnostic, namely, X-ray, Computer Tomography(CT), MRI, Positron Emission Tomography(PET), Mammogram, Ultrasound, Fluoroscopy and Cerebral angiography [12], [13], [14].

### **I. X-ray**

X-rays make images by introducing a little amount of radiation into the body. The radiologic technician must first make sure the patient isn't covered in jewellery or wearing anything too tight to prevent image quality degradation. The patient must next be placed in the proper position. After all of that is taken care of, it's time to photograph what's going on within the body [25].

### **II. CT**

The CT scanner is a big donut-shaped machine that takes images while the patient travels through the centre. For some exams, the patient may receive an oral contrast agent or an injection of contrast agent to help show what's happening inside the body. The technologist places the patient on the scanner bed and then exits the room once everything is ready. The patient is carefully moved across the centre of the scanner by the technologist from a control room [26].

### **III. MRI**

Organs and tendons are examples of soft tissues that respond well to MRI imaging. Unlike CT scans, MRIs rely on radio waves and magnetic fields rather than ionizing radiation. On a table with a tube attached, patients lie down. The technician positions the patient

such that the magnet is above the bodily portion being examined. During the examination, the patient and the technologist can communicate thanks to two-way transmitters [27].

#### IV. PET

A PET scan, also known as a positron emission tomography scan, is similar to a test used to diagnose diseases in humans because it can spot problems at the cellular level. Radioactive tracers are injected into the body as part of the process. The tracers employ a PET scanner to discover issues that could otherwise go unnoticed until they get worse [28].

Tracers can be administered in one of three methods, depending on the procedure, through injection into a vein, gas inhalation, or drinking a specific concoction. There is a one-hour delay before the scan can begin since it takes tracers a long to move throughout the body. When the time is appropriate, the patient will lie down on a table that moves through an O-shaped machine. The patient receives directions from the technician on when to hold their breath and when to be still [28], [29].

#### V. Mammogram

Two types of mammograms namely, screening and diagnostic mammograms. Mammogram is mostly used in breast cancer detection. First, any anomalies are found using screening mammography. Following the discovery of thickening in the breast, diagnostic mammography looks for cancer. The fight against breast cancer depends on early cancer detection [30]. The best practices used by technologists will vary depending on whether a screening or a diagnostic exam is being performed. During screening exams, each breast is often the subject of two photographs. However, diagnostic tests are longer and include the technician capturing more images from more perspectives. In order for doctors to inspect problematic locations, magnified images are also taken [31].

#### VI. Ultrasound

An ultrasound, also referred to as a sonography, employs high-frequency sound waves to record images from inside the body. It is frequently used to find problems with soft

tissues including organs and blood arteries. Ultrasounds are the method of choice for examining pregnant women because they are radiation-free [32].

The way to get ready for an ultrasound depends on what will be looked at. Patients must fast before tests anywhere near the abdomen, but water may be consumed. A lubricant is given to the skin as the patients are lying down on an examination table. High-frequency sound waves are sent into the body by a device known as a transducer as it glides over the skin. These sound waves produce an impression of bodily motion [32].

## VII. Fluoroscopy

Certain examinations can be compared to photography, a fluoroscopy is more like a moving image of the body's activity. This is so that you can see moving bodily parts on a fluoroscopy. Contrast dyes are frequently used throughout the surgery to demonstrate how they move through the body. A monitor receives signals from an X-ray beam while all of this is going on. Fluoroscopies are used to check both hard and soft tissue, including arteries, joints, organs, and bones. Fluoroscopy is frequently used in blood flow exams [33].

First, the technologist places the patient on the examination table. The patient may be asked to move during the fluoroscopy in contrast to many other exams when the patient is instructed to remain immobile in order to better understand how the body is responding to motion. Although fluoroscopy itself is not difficult, injecting contrast dyes into the body can be painful, therefore technologists may need to offer comfort measures [34].

## VIII. Cerebral angiography

This invasive examination creates images of the brain's blood arteries using x-rays and a contrast agent that contains iodine. It can offer more details about the abnormalities seen in a head MRI or CT scan [35].

This study uses MRI scanning as its imaging modality and makes use of a number of MRI acquired datasets. More specific information regarding the physics and operation of MRI is provided in the following section.

### **2.3.1 Magnetic Resonance Imaging**

The inside anatomy of the body can be seen using the medical imaging technology known as MRI [27]. The foundational ideas of Nuclear Magnetic Resonance (NMR) are utilized in this method. Using radio waves and a strong magnet connected to a computer, a method known as NMR produces comprehensive images of various bodily regions that may distinguish between normal and diseased tissue [36]. MRI gives great detail, making it possible to examine soft tissues like the brain using it. It has the ability to identify minute variations, even between similar locations, unlike CT scans, which are effective for imaging bone and soft tissue but offer less detail [27]. An MRI can commonly detect brain abnormalities that are too small or located in regions of the brain that a CT scan cannot properly identify. The non-invasiveness, adaptability, MRI with strong flow and diffusion sensitivity and good tissue contrast are some of its main advantages over conventional medical imaging methods [27], [36].

In MRI, strong magnets are employed to create a magnetic field that is so strong that it compels the body's protons to adhere to it. When an RF current is delivered into the patient, the protons are forced against the magnetic field's pull and spin out of balance [27]. When the RF field is turned off, the MRI sensors may be used to detect the energy created when the protons realign with the magnetic field. The surroundings and the chemical composition of the molecules affect how much energy is produced and how long it takes the protons to adjust to the magnetic field.

Using these magnetic characteristics, medical professionals can distinguish between different tissue kinds [36]. The subject of an MRI scan is placed inside a huge magnet, and great stillness must be maintained during the imaging process to prevent visual blur. Before or during the MRI, a patient may receive intravenous contrast agents often containing the element gadolinium to expedite the rate at which protons realign along with the magnetic field. When the image is more vivid, the protons realign more quickly [27], [36].

MRI utilizes the spin of the proton, a subatomic particle with quantized angular momentum, as well as other quantum mechanical features of subatomic particles. Since the majority of the human body is made up of fat and water, this feature can be employed in medical applications to measure hydrogen levels [36]. In fatty tissues and water, there is just one proton per hydrogen atom. When this spin encounters an external magnetic field, it generates a net nonzero spin and develops a magnetic moment, at which point it aligns with the exterior environment [37].

When there is no magnetic field, hydrogen's magnetic instant is randomly distributed, and there is no net magnetic field. The atoms will line up themselves beside the field's flux lines if a  $B_0$  external magnetic field is supplied.  $B_0$  is the energy input in rotating magnetic field. The magnetic moment it encounters at  $B_0$  will cause it to travel through a secondary spin in addition to its primary spin. The magnetic moments follow a cyclical processional journey at the processional frequency speed, also known as the Larmor frequency, as a result of this secondary spin, which is known as precession [36], [37].

### **2.3.2. Magnetic Resonance**

When external energy is introduced into a nuclear spin system close to the Larmor (resonance) frequency, magnetic resonance results. The main energy input in both NMR and MRI is a rotating magnetic field called  $B_0$  produced by supplying alternating current via a nearby radiofrequency(RF) coil [18]. Figure 2.1 shows a schematic representation of NMV both prior to and following the delivery of an RF pulse to MR active nuclei.

When the hydrogen magnetic moment is positioned along the same route as the procession around the magnetic field  $B_0$ [28], phase coherence occurs at resonance. As a result, in the X-Y plane, transverse magnetization is a superimposed magnetic vector, as seen within Figure 2.1.



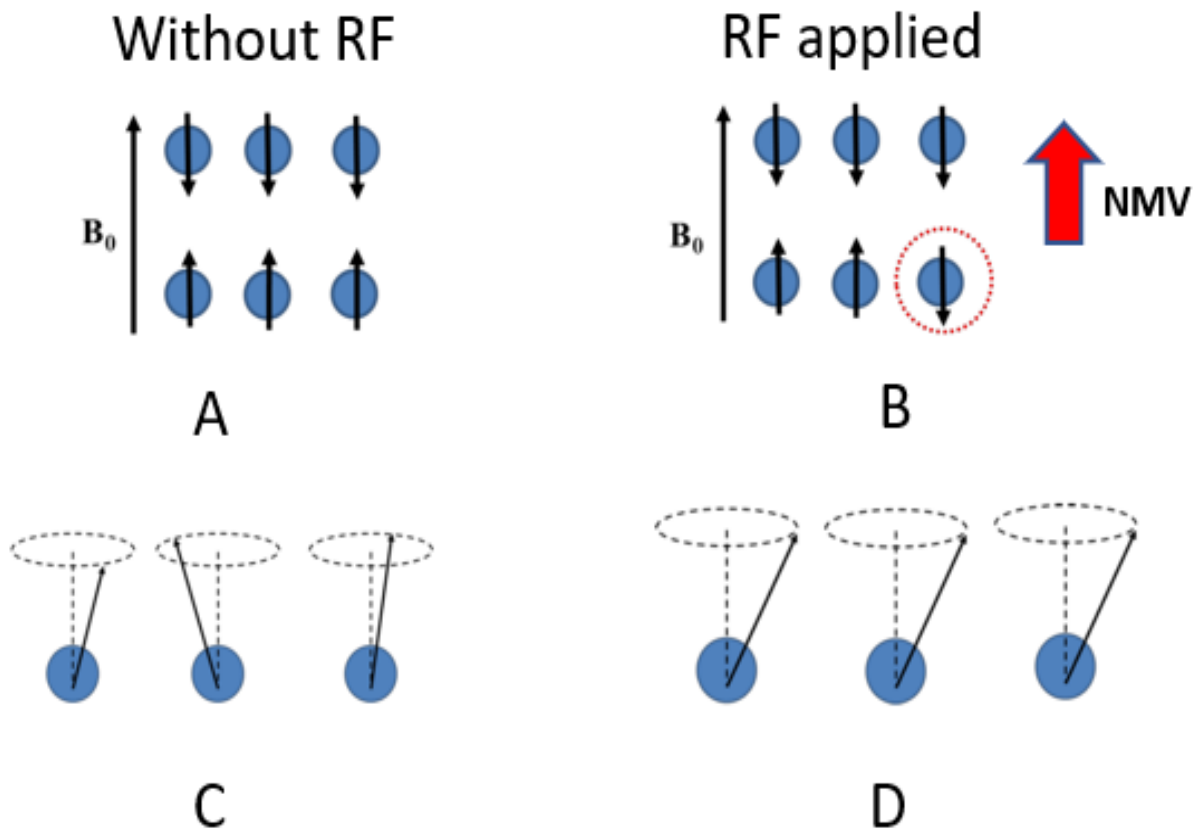


Figure 2.1 The outcome of applying an RF pulse when the atoms are exposed to an outside magnetic field [28].

Without using an RF pulse; (B) while using an RF pulse, which leads to a rise in the number of both an NMV and high-energy spin-down nuclei. When an RF pulse is present, phase coherence (C) is out of phase or incoherent. Once the RF pulse is administered

the Larmor frequency (38), (D) illustrates phase coherence that is coherent or in-phase.

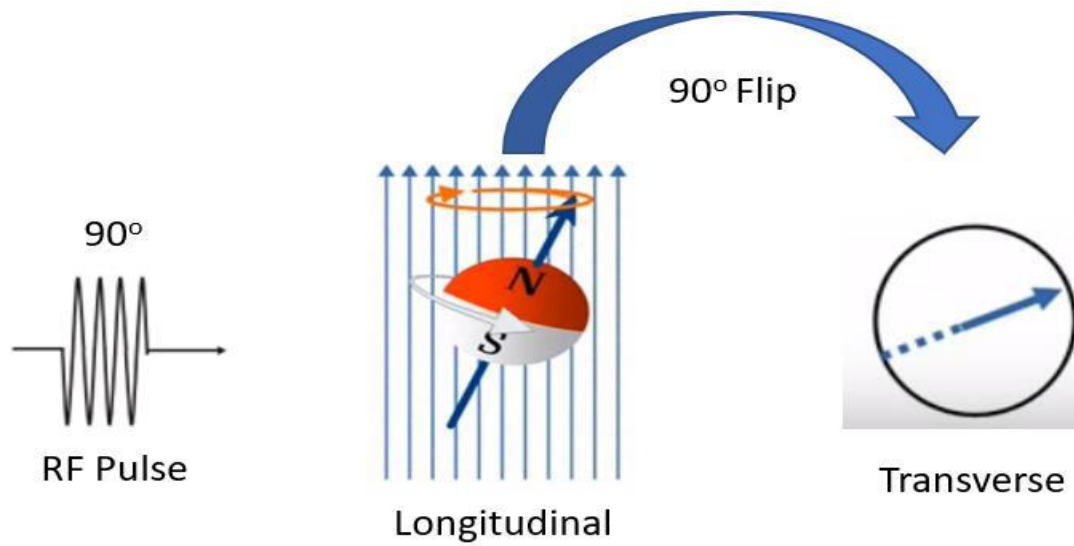


Figure 2.2 The use of a radio frequency energy pulse to ignite a magnetic nucleus [38].

A sample or target tissue is subjected to a strong, continuous magnetic field to produce the MR signal [38]. The degree of magnetization in the cross-sectional plane affects the signal's strength. The signal's frequency and the Larmor frequency are same. The NMV makes an effort to adjust to the magnetic field of the environment  $B_0$  in this circumstance since the nuclear energy obtained by the RF pulse will be lost once it is terminated. The recovery phase is characterized by an increase in the longitudinal magnetization, which has exponential features. The decay phase, which occurs concurrently, is marked by an exponential decline in the magnetization in the transverse plane. When the amplitude of the induced voltage inside the receiver coil decreases, a free induction (FID) signal is consequently generated as the decay progresses [38], [39].

### 2.3.3 Relaxation

Relaxation is the process of how signals evolve over time. The excitation energy that the hydrogen nuclei absorbed during the RF application is lost during the relaxation period. As a result, hydrogen nuclei's magnetic moments are rendered noncoherent, and the NMV returns to the starting of  $B_0$ . The hydrogen atoms relaxation times vary and are

frequently two measurements: once for the prolonged relaxation, sometimes called T1 recovery, and once for the transverse relaxation, usually called T2 decay [40]. The relaxing process is shown in Figure 2.3.

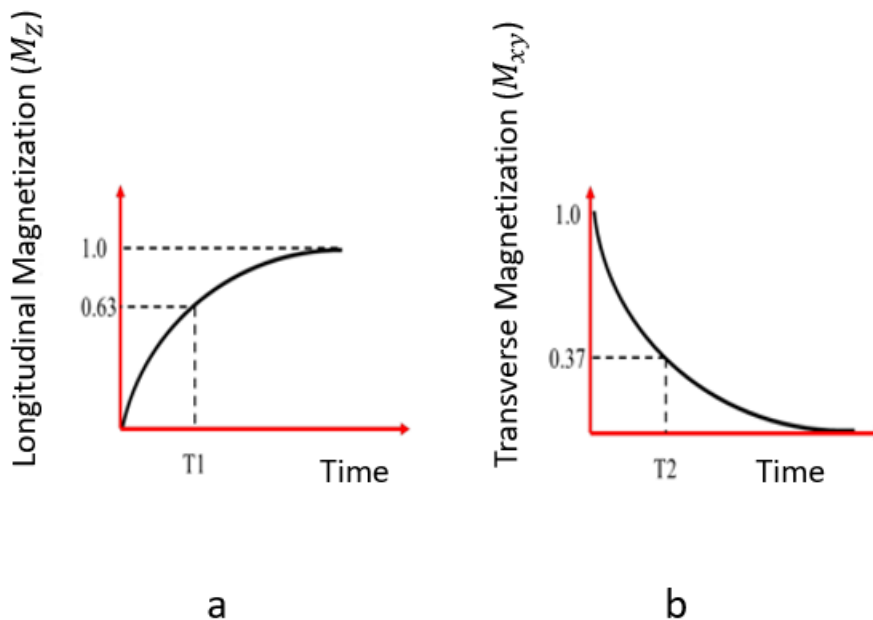


Figure 2.3 T1 recovery curve in (a) and T2 delay curve in (b) [40].

The process connected to T1 is what causes the signal to become less intense [40]. The magnetic moments of nuclei regain their longitudinal magnetization as a result. T1 is influenced by the magnetic field intensity and tissue characteristics. A distinct procedure associated with T2 is what widens the signal[41]. When the nuclei transmit energy to the nearby nuclei, T2 decay takes place. Spin-spin relaxation, which is also known as the loss of magnetization in the transverse plane during decay [42]. T2 generally recovers 5 to 10 times more quickly than T1 and is influenced by the characteristics of both the magnetic field's strength and the tissue's porosity [40]. The strength and signal-to-noise ratio of the signal are influenced by the magnetic properties of the tissue under scan that is the target. The significant proton concentration of magnetic nuclei within the tissue, along with its short T1 and extended T2 times, for a certain set of imaging parameters, may increase the signal-to-noise ratio [41]. Aside from hydrogen nuclei, the biggest drawback of imaging nuclei is the faint signal they produce due to the low tissue concentration [40],

[41]. Echo time (TE) and Repetition time (TR) are often utilized in imaging modalities to control signal strength and contrast. These two factors must be considered while selecting the parts for a certain imaging procedure. Longitudinally magnetization not being able to maximize and provide a strong signal strength if a T1-weighted picture is created using a short TR [42]. In addition, if the TR is lowered to speed up image capture, image noise ends up being the bottleneck. Long TE values may also cause the signal produced by the transverse magnetization to drop to incredibly low levels [42].

#### **2.3.4. Conventional MRI Protocols (Conventional MRI)**

The Repetition Time (RT) and Time to Echo (TE) parameters of tissue are used to create the C-MRI protocols (TR). This section provides an explanation of the intricacies of C-MRI acquisition [43].

##### **2.3.4.1 T1 Weighted Image (T1WI)**

When the TE and TR are both brief, a T1-weighted protocol is captured. T1-weighted imaging will highlight tissues with short T1 values, which is important from a clinical standpoint. This procedure typically results in better contrast between liquids, tissues made of water, and tissues made of fat. Brain imaging, this approach provides strong contrast between GM and WM [43], [44]. Three distinct tissue types namely, brain tissue, CSF, and fat will be easy to distinguish with a TR value that is only about 500 ms. The GM and WM of the brain are visible with medium intensity in a T1-weighted image, while fat exhibits appreciable hyper-intense values. The CSF appears hypo intense. Injecting contrast agents into the patients may also aid in boosting specificity by creating numerous images with various contrast levels [44].

Contrast-enhanced T1 weighted

Gadolinium-based contrast agents (GBCA) are given during 3D spoiled gradient-echo (GE) sequences used in contrast-enhanced MR Angiography (MRA) [44]. Almost any region of the body's vascular architecture can be evaluated with it. Its primary attributes are:

- I. T1 weighted spoiled gradient-echo sequence (T1-weighting is permitted for flip angles between 25° and 50°)
- II. The arterial phase of the study's central k-space acquisition optimizes the preferred visibility of arteries.
- III. Use of GBCAs to reduce the blood's T1 interval, which makes the blood seem bright.

#### **2.3.4.2 T2 Weighted Image**

When TE and TR are both long, a T2-weighted process is produced. This method enables accurate differentiation of scalp fat and several brain regions (including the GM, WM, and CSF) for brain tissue T2 values [45]. Longer T2 times are a result of faster spin interactions and in tissues with more mobility, the fluid portions exhibit slower transverse coherence loss. Additionally, for smaller structures like those that have a lot of cells, a shorter T2 time is created by longer spin interactions and a quicker loss of transverse coherence. Fluids are frequently shown as particularly bright in T2-weighted scans, whereas tissues made of water and fat are shown as being mid-grey [46]. The damaged tissue's T2 values are prolonged by brain lesions, which frequently result in structural damage to the brain [45].

#### **2.3.4.3 Fluid Attenuated Inversion Recovery (FLAIR)**

When the T1-weighted Images' dynamic range is increased with a 180 RF pulse rather than a 90 RF pulse, a fluid attenuated inversion recovery (FLAIR) picture is created [36]. All of the tissue beneath B0 has its longitudinal magnetization completely inverted by an RF pulse known as an inverting pulse.

The magnetization thus starts out negative and declines until it approaches zero [47]. The FLAIR procedure is the most popular method for identifying non-enhancing lesions in the cerebral vasculature because it produces a CSF signal loss on a T2-weighted scan. A few C-MRI pictures of a cerebrovascular illness are depicted in Figure 2.4.

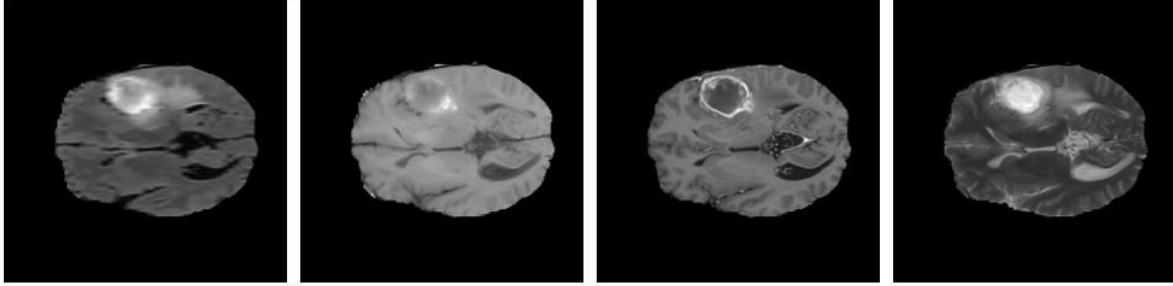


Figure 2.4 Examples of C-MRI pictures of a cerebrovascular disease include FLAIR, T1-weighted, T1-contrast, and T2-weighted images (from left to right) [36].

## 2.4. Diffusion Magnetic Resonance

One of the most crucial modern MRI methods in neuroradiology is diffusion imaging [48]. The notion of diffusion is defined in the following section, which also explains how water molecule diffusion in the brain structures produces MR pictures.

Contrast in the images produced by diffusion-weighted imaging (DWI) MRIs is not similar to that of traditional MR techniques. In particular, DWI can distinguish cerebrovascular from other processes that occur with abrupt neurological impairments and is sensitive to the identification of cerebrovascular disease [49]. DWI is a type of MRI that gauges the water molecules random Brownian motion within a tissue voxel. This generally means that tissues with a high cell density or tissues that have cellular edema have lower diffusion coefficients. It is possible to infer details about cellular tissue organization using the DWI approach based on water motion. It is believed that the distribution of water molecules that diffuses over a specific period has a Gaussian shape, with a breadth proportional to the ADC [48]. The imaging gradient's sensitivity to diffusion is influenced by its intensity, direction, and temporal profile, all of which can be distilled down to just one  $b$  number. The tissue's water evaporation behaviour can then be identified by creating a parametric map using images taken at various  $b$ -values [50]. The pertinent echo attenuation in a voxel in this scenario could be expressed as follows:

$$S(b) = S_0 e^{-bADC} \tag{2-1}$$

where  $S$  represents signal strength and The diffusion weighted imaging parameter  $b$  can be obtained using the following formula:

$$b = \gamma^2 G^2 \delta^2 (\nabla - \delta^3) \quad (2-2)$$

where  $G$  denotes the gradient's force, the gyromagnetic ratio, the separation between gradient lobes, and the length of the diffusion-encoding gradient lobe. In order to track the thermal mobility of the water inside and around the cells, bipolar gradient coils are triggered and their amplitude and intensity are controlled by the  $b$  values (Brownian motion). The typical anatomical pictures may be overlaid with the ADC map to understand more about the tissue being studied [50]. The most common  $b$  values to create the best balance of tissue diffusion and signal are 500 and 1000, as shown in Figure 2.5.

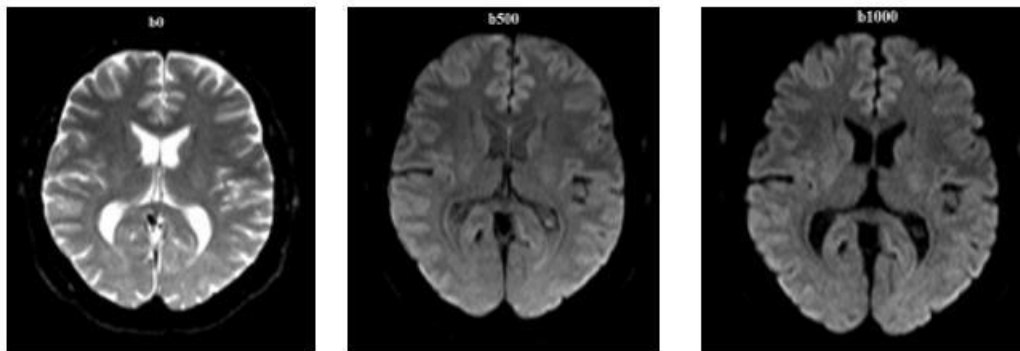


Figure 2.5 DWI of different  $b$  value [50].

## 2.5 Dataset

The CNN model that was used to identify cerebrovascular disease in this study was implemented using an MRI publicly accessible dataset. Brain images using MRI was obtained from Kaggle public dataset. The dataset was divided into two folders, infected and not infected images. The dataset consists of 253 images where 155 are infected images and 98 are not infected images.

## 2.6 Conclusion

The history of cerebrovascular disease was covered in this chapter. Additionally, a review of MR methods used in cerebrovascular was done. A complex MRI modality was described, and the C-MRI acquisition techniques were covered. Additionally, a description of the publicly accessible datasets used in this investigation was provided.

## **CHAPTER 3: LITERATURE REVIEW**

### **3.1 Introduction**

A review of the literature is presented in the first section of this chapter, which is followed by a discussion of the approaches that are pertinent to the issue at hand. Cerebrovascular disease detection in MRI images is another topic covered in this chapter. We evaluate and thoroughly investigate the proposed automatic methods for the detection of cerebrovascular disease in MRI images. Along with pertinent research on the segmentation of lesions, this chapter also provides the protocols for evaluating the method for certifying the results of segmenting MRI images.

### **3.2 Segmentation of MRI Images for Detection of Cerebrovascular Disease**

The most crucial stage in almost all detection projects is the segmentation of MRI images, without it, there would be no Region Of Interest(ROI). To minimize the complexity of an image and facilitate future processing or analysis, The process of breaking down a digital image into multiple subgroups known as image segments is called image segmentation [49]. The segmentation of the cerebrovascular system in MRI images has been studied using a variety of approaches. The segmentation of MR image features is challenging because uncontrollable factors like the amount of contrast agent and the duration of the acquisition may change how the ROI appears in the image and cause the same tissue to appear with various intensities [50]. According to how much human involvement is necessary, picture segmentation can generally be divided into three categories, manual, semi-automated, and fully automatic [51].

A specialist, frequently a radiologist or other skilled physician, does manual segmentation in the majority of cases [3]. Slice by slice is typically used, however it is also possible to do this in 3D by having the expert either encircle the ROI or annotate the voxels of interest. The capacity to use expert knowledge is a benefit of this segmentation method, but it also has the disadvantages of being time consuming and subject to intra- and interobserver variability. As a result, even though manual segmentation is frequently regarded as the



gold standard, there can be significant variations in the derived radiomics values due to this variability [49], [51].

Semiautomatic segmentation aims to address some of the issues associated with manual segmentation. For instance, by expanding the segmentation to other slices or growing the segmentation over a region to do away with the necessity for slice-by-slice segmentation, less human work and time is needed [52]. There are many different semiautomatic approaches, and some algorithms help during or even before the segmentation while others aid in the segmentation's completion [53]. Additionally, initial semi-automatic algorithms try to lower the variability between observers. Interobserver variability will still exist, though, because the segmentation's manual component and the algorithm's settings have an impact on the outcome [54].

Automatic segmentation techniques fall into two categories learning-based and non-learning-based, and neither requires user interaction. Deep learning, a learning-based approach, has recently gained a lot of popularity. In this approach, a neural network that has been trained using labelled samples does segmentation. The U-Net architecture is a well-liked deep learning strategy. The benefit of this strategy is that the segmentations may be completed quite rapidly after the mechanism has been developed. This can take seconds to minutes, depending on the image, but it normally happens considerably faster when user contact is necessary [54], [55].

Deep learning has the drawback of typically requiring a large amount of labelled data, a lengthy training period, and specialized technology to build the model. These techniques frequently use segmentations from a single observer, which means that the resulting model will share the observer's bias. Since an algorithm that has been taught on one dataset may perform very poorly on another, learning-based techniques may not generalize well. Additionally, semiautomatic or manual segmentation techniques must still be utilized for the training data segmentations [53], [54], [55].

Unsupervised segmentation algorithms take advantage of image-based traits like intensities. These techniques can handle more complicated cases. There are four different types of techniques: approaches for classifying pixels, threshold-based methods, region-

based methods, and model-based methods. The two main categories of cerebrovascular segmentation techniques used in this study are: approaches for picture segmentation based on semantic classification [56].

### **3.3 Image Object Classification-Based Methods**

The goal of this technique is to categorize or forecast the class of an object in a picture. The main goal of this technique is to precisely to determine an image's features.

In supervised classification, a group of example items with known classifications are provided, and experts select the classes to which an object may belong. The classification algorithm employs this group of well-known objects as a training set to learn how to categorize things. Unsupervised classification approaches do not require training sets or pre-defined classes. The initial phase of classification involves training the algorithm on the training dataset. A labelled test dataset is used to verify and assess the extracted model's performance and accuracy [55]. The categorization techniques typically need the following steps, a dataset with predetermined labels is gathered in the first step, the labelling of medical imaging is typically visible and may be completed after inspection by an expert operator [55], [56]. The processes for data pre-processing and data preparation is the second step. Algorithms for pre-processing can be used to solve problems like omitted values, discretization, and noise removal.

In the third step, features that are unnecessary or redundant are found and eliminated using feature selection. The algorithms become faster and perform better as a result. Selecting the learning algorithm is a crucial step. Evaluation is the last action. In this context, there are at least three ways to assess classifier accuracy, all of which depend on splitting the data into sets for training, validating, and testing. These three datasets are split from one another differently by each of these strategies [57].

The most widely used algorithms for cerebrovascular segmentation are methods that require a labelled training dataset are supervised procedures. The size and calibre of the dataset's labelling a laborious task directly affects how accurate the procedure is. The trained model is fed the testing dataset during the testing phase. The voxels in the MR image are then allocated to a class because the results of the detection approach are

crucial for strategizing the treatment of cerebrovascular disease, it must be particularly accurate. A discrete probability distribution is generated using a model based on picture classification [57]. The model has been taught to identify the characteristics of each class. High-level features generated automatically are used in other classification-based models for images, while other classification-based models train using hand-crafted designed features. The following section discusses both manually constructed feature approaches and deep learning feature methods.

### **3.3.1 Customized Feature Methods**

Over the past ten years, numerous automatic ROI segmentation techniques have been presented. The customised features approach is used in the majority of automated brain ROI procedures. The detector is either a random-decision forest (RF) or a support vector machine (SVM), whose feature type is unaffected by the training procedure. Local histograms, Gabor, and area shape difference are part of the initial feature extraction process. Gathering features from the pictures, customised feature segmentation algorithms create models based on how the characteristics relate to different classes of pixels and voxels [58].

The features are first extracted in the pipeline of traditional machine learning, and then they are provided to the chosen detector. As long as the input features have a strong enough ability to discriminate between healthy and unhealthy tissues, the detector is trained to do so. These characteristics could include histograms, the texture of the photographs, and the intensity values of the raw input pixels. In many situations, it has been demonstrated that a linear kernel performs well and only has to have one parameter tuned. Without dividing the tissue subtypes into segments, their approach can detect the entire cerebrovascular ROI. The fact that the hand-crafted features typically require calculating several different features, which slows computation and raises memory costs, is one disadvantage of them [58].

#### **3.3.1.1 Decision Trees**

Using a set of guidelines or questions on the qualities of the class, a decision tree is utilized to categorize classes using a hierarchical tree structure. The training set's feature

space is recursively divided to produce a decision tree. To construct a reliable and informative hierarchical classification model, a collection of decision criteria that naturally segment the feature space must be identified. For both classification and regression issues, a decision tree is a type of model that resembles a tree [54], [55]. By dividing the training set and utilizing the information gain, the split function parameters are modified at each node of the decision tree during training. The testing procedure comprises applying the tree's feature vector to each node until a leaf node appears using the testing data's feature vector. Due to its inherent ability to manage multiclass problems and huge feature vectors, this approach is currently widely employed. The algorithm was created as a supervised technique for segmenting brain illnesses. As additional input, decision tree classifiers are trained in this stage using probabilities derived from tissue-specific Gaussian mixture models. Author [59] proposed a similar strategy, but theirs makes use of an exceedingly random tree classifier in order to make use of the variety of attributes when separating the trees.

### **3.3.2 Methods for Deep Learning Feature**

When developing Adaptive characteristics for tasks of picture segmentation applications like brain illness segmentation, deep learning techniques are frequently used. Creating feature representations that are task-adapted is possible using the deep learning approach, which directly builds a hierarchy of increasingly sophisticated features from information gathered within the domain. Deep learning-based features usually outperform hand-engineered features in terms of performance [59].

#### **3.3.2.1 Convolutional Neural Network Layers**

Supervised visual models using convolutional neural networks that may be taught to detect incredibly minute differences between features of varying degrees of complicated. CNNs are multilayer feedforward structures that are effective in a range of visual tasks, such as segmentation, recognition, and detection. One to three layers or stages make up CNNs in most cases. A convolutional filter bank layer makes up each level, a spatial feature layer, and a nonlinear transform layer or down-sampling. Local characteristics from the input picture are gathered and integrated in sequenced layers during training

(learning) to produce a higher order architecture [60]. To use the training technique to infer the label instances in the training set, the kernels and connection weights for each layer must be learned. A collection of integrated and specifically designed filter banks (kernels) for the job at hand are the procedure's results. Recently, CNN-based algorithms outperformed more conventional classification techniques in their ability to learn the characteristics of hierarchies. Deep neural networks are built using CNNs because they are built from numerous blocks that are piled high of one another to generate a hierarchy of attributes. Convolutional and non-linear activation function (ReLU), which are the two main layers that make up these blocks, are followed by pooling layers. Up until a particular size is reached in the picture, these blocks are repeated in accordance with the pattern that has been selected. The final block, which is coupled to the supplies the class label with fully convolutional layers (FC) [61]. These blocks' design enables a wide range of architectural options. A group of CNN layers are briefly explained in the section that follows:

### I. Convolutional Layer

A crucial component of a CNN is a convolutional layer. The filter kernel is a set of weights that connects the filter kernel's constituent units to the local patches of the layers that came before it. The user must comprehend the hyper-parameters for the kernels' width and height. The output of a convolutional layer is produced by convolving the current layer's kernel with the outcomes of preceding units. In deep networks with multiple convolutional layers and different network routes, a suitable weight initialization is crucial [61]. The output of each convolutional layer is a feature map. The output volume is obtained by concatenating each of the third dimension, followed by these filter maps. The convolutional layers positioned below the various input array dimensions reduce the filter response dimension.

### II. Non-linear Activation Function

To create non-linear characteristics modifications of the input, The outcome of the kernel convolution is subjected to an element-wise non-linearity. The ReLU is the most used nonlinear function defined by the following formula [61]:

$$f(z) = \max(z, 0) \tag{3-1}$$

ReLU is a good option for use in deep learning procedures since it can learn more quickly in networks with several layers.

### III. Pooling Layer

The network can be made to be invariant to the local fluctuations of each feature level by subsampling feature maps, which are thought of as a pooling layer, and the X and Y axes' spatial dimensions. In addition to decreasing the output dimensionality and parameter numbers, the pooling layer renders the network insensitive to minute changes in every level of input in the preceding layers [62]. Other research suggest that pooling layers won't even be needed at all in next CNNs [63]. The most popular pooling technique, max-pooling, chooses the highest values from each feature map. An illustration of the well-known max-pooling layer window with stride 2 and filter size 2 is shown in Figure 3.1.

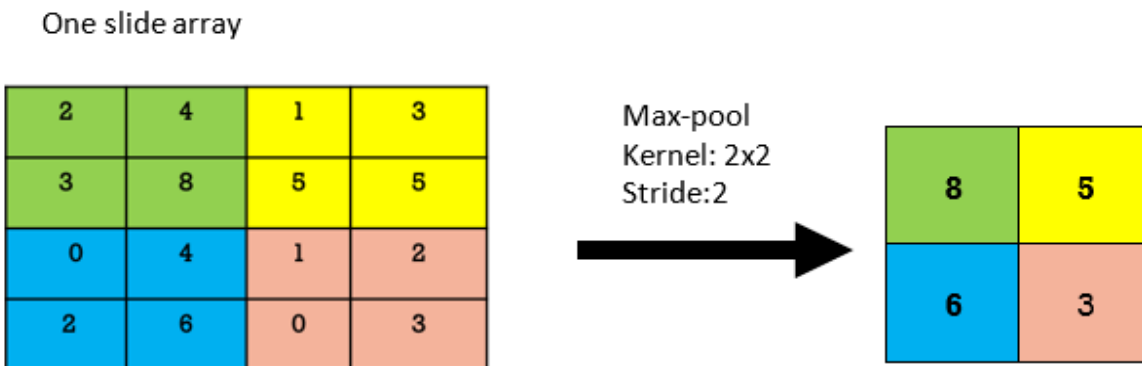


Figure 3.1: Example of maximum pooling using a 2x2 kernel and 2 stride.

### IV. Fully Connected Layers

Fully connected layers are used by the neural network to construct the data class after numerous convolutional and max pooling layers (FC). Each neuron has a different set of connection weights between every hidden FC layer unit and every covert object in the layer above. Given that the units are spatially coupled to the input area, this has an effect on the CONV layer [63].

### **3.4 Semantic Object Segmentation-Based Approaches for Images**

The process of categorizing each pixel as belonging to a specific label is known as semantic segmentation. Semantic segmentation requires a deeper understanding of the image. Both the presence of items and the pixels corresponding to each object should be determined using the algorithm. The complex visual models known as fully convolutional networks (FCNs) are based on the semantic segmentation of images. It has been demonstrated that FCNs perform at the cutting edge of semantic segmentation [64].

FCNs can be fully trained for pixel-wise prediction within the transition from broad to specific prediction. FCNs are capable of predicting dense outcomes from inputs of any size. Learning and inference are conducted simultaneously on the entire image using computing with dense feed-forward and reverse propagation [64].

#### **3.4.1 Architecture for Fully Convolutional Networks (FCN)**

The Fully Convolutional Networks (FCNs) architecture is best utilized for semantic segmentation. For the segmentation of visual semantics, the FCN method was suggested. This technique alters the architecture of CNN. A Skip layer was initially built in between them to connect the deeper sharper visual information from the shallow levels combined with semantic information from the layers. The output's spatial accuracy and semantics are improved by the Skip architecture. Instead of a pooling layer, the second update develops dense prediction using an up-sampling method. In order to enhance CNN's last layer for semantic segmentation, convolution techniques have been proposed. It is possible to migrate different CNN networks to FCN. The FCN architecture's highest performance and outcome were experimentally attained by the VGG 16 network [63][64]. So, in the current investigation, this network was utilised.

#### **3.4.2 U-net Architecture**

U-net is a well-known network that is used for semantic segmentation or classifying pixels of an image so that they are assigned labels according to the class they belong to (for example, a human). The fundamental idea is to add additional layers to a typical contracting network where up sampling operators are used in place of pooling operations. Thus,

the resolution of the output is increased by these layers. Furthermore, depending on this knowledge, a succeeding convolutional layer can learn to put together a precise output [65].

There are a lot of feature channels in the up sampling phase of U-Net, which is a significant change that enables the network to convey context information to higher resolution layers. As a result, the expansive path produces a u-shaped design because it is roughly symmetric to the contracting component. There are no fully connected layers in the network, it just utilizes the valid portion of each convolution. The missing context is extrapolated by mirroring the input image in order to forecast the pixels in the border region of the image. To apply the network to huge images, this tiling technique is crucial since, without it, the GPU RAM would constrain the resolution [66].

Figure 3.2 depicts the network architecture, which is made up of 23 levels. There are two primary routes in the U-net: an expanding route, and a contracting route. The purchasing procedure follows CNN's established architecture. A ReLU follows each of the two convolutions of 3x3 that are present on this route. A kernel size-based max-pooling layer of 2x2 and a downscaling stride of 2 is present in each block of the design. At each step of the U-expansive net approach (on the right), the feature map is up-sampled before being convoluted with a 2x2 kernel size, or up-convolution. The feature map from the contracting path that was chopped is added to the feature maps. Two 3x3 kernel size convolutions and two ReLUs are then placed after them. Each feature vector component is translated to the predicted number of classes using a convolution with a 1x1 kernel size in the final U-net architectural layer [64].



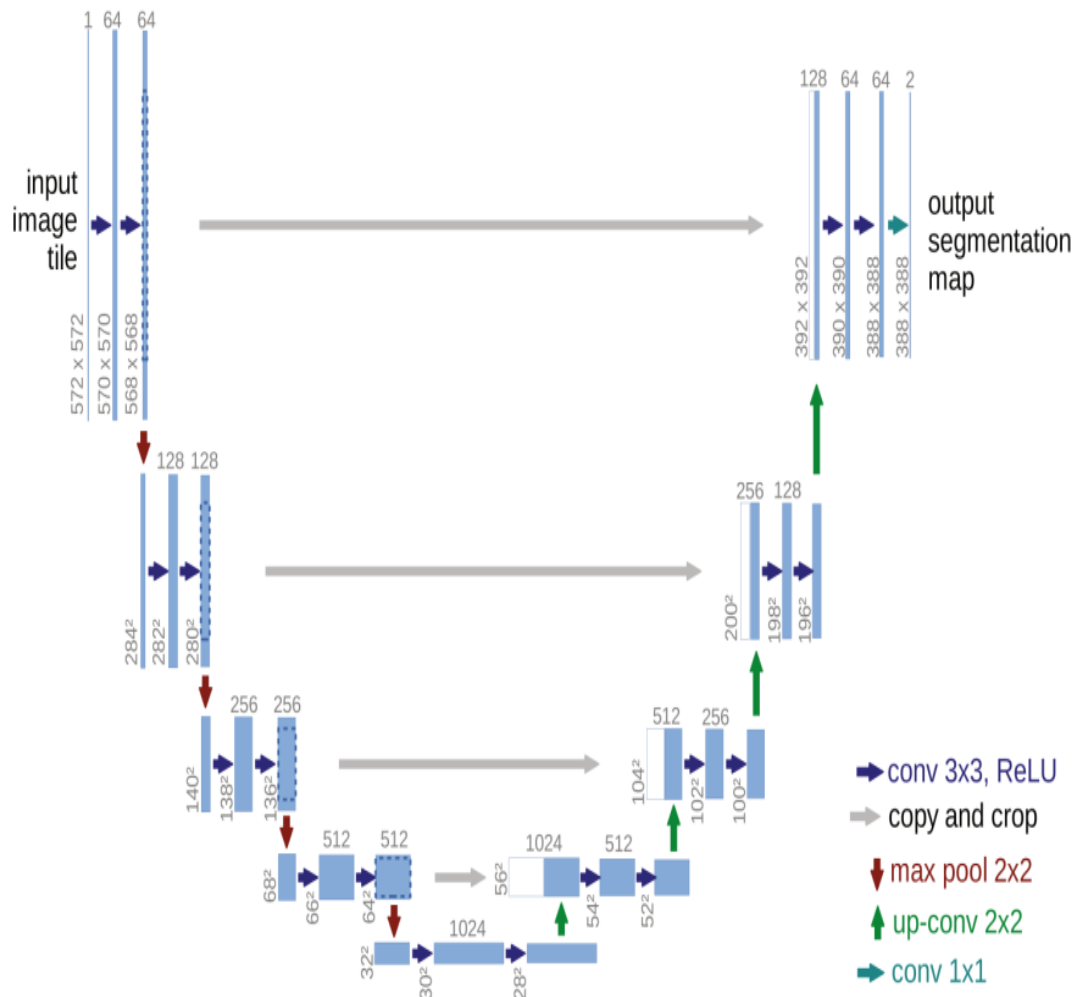


Figure 3.2 U-net design example with the lowest resolution of 32x32 pixels [64]

### 3.5 Measurement Metrics

Classification in machine learning refers to the process by which a computer uses an algorithm to draw conclusions from previously known data and then applies those conclusions to fresh data. In particular, it enables intelligent decision-making in the fields of machine learning, pattern recognition, and data analysis. Although there are many different classification schemes, binary and multi-class classifications are the two that are most frequently employed in illness detection. When performing binary classification tasks, one class stands in for the normal state, while the other represents the abnormal state. When performing multi-class classification tasks, either one class must fall inside a category that

is known to exist [66]. The training data, which includes both the input and intended outputs, must consist of a sample of observations and measurements for which the target value is already known in order to employ the supervised classification approach. A diagnostic test's ability to distinguish between those who have an illness and those who do not determines how accurate it is [67].

Patient's test results are classified as positive or negative, with positive indicating the presence of a disease and negative indicating the absence of an illness. False positive (FP) observations are those in which the expected class is positive but the actual class is negative. True negative (TN) observations are those in which the expected and actual classes are both negative. True positive (TP) observations are those in which the expected and actual classes are both positive. False negative (FN) observations are those where the expected class is negative but the actual class is positive [68][69].

### **3.6 Related Works in Detecting Cerebrovascular Disease**

Cerebrovascular disease is the second world's major factor in mortality and disability [1], and the fourth major cause of mortality and disability in South Africa [2]. Blockage of blood flow to the brain is the primary cause of cerebrovascular disease. The existing studies on cerebrovascular disease detection used binary method which uses pixels to decide if the patient have the disease or not and morphological operation which uses erosion and dilation. However, both methods do not show any maturity of the disease by providing accuracy percentage and confusion matrix which may help in interpreting the images, therefore, both methods don't outperform human beings since they don't provide more information about the disease [9]. Other studies on cerebrovascular disease developed a logistic regression model that predict the cerebrovascular disease given basic symptoms like age, sex, hypertension etc[14]. Another study developed a robotic arm to predict the presence of cerebrovascular disease by putting the robotic arm on the hand, however, both methods do not scan the body to check damages on the brain leading to possible false positives and false negatives [15].

### 3.7 summary of related works and gaps

Article name	Author	Shortcomings
Fully convolutional networks for semantic segmentation.	Long, J.	Deep learning has the drawback of typically requiring a large amount of labelled data, a lengthy training period, and specialized technology to build the model. These techniques frequently use segmentations from a single observer, which means that the resulting model will share the observer's bias. Since an algorithm that has been taught on one dataset may perform very poorly on another, learning-based techniques may not generalize well.
Cerebrovascular accident prediction using logistic regression algorithm.	Geeth, M., Radhika, P., Priya, S., & Latha, S.R.	This study developed a logistic regression model that predict the cerebrovascular disease given basic symptoms like age, sex, hypertension etc, however, the method do not scan the body to check damages on the brain leading to possible false positives and false negatives.
Robotic arm for cerebrovascular accident patient by using Wi-Fi module.	Poovarasana, B., Sudher-son, M., Sundarakrishnam, D., & Sureshkumar, S.	This study developed a robotic arm to predict the presence of cerebrovascular disease by putting the robotic arm on the hand, however, the method does

		not scan the body to check damages on the brain leading to possible false positives and false negatives.
Segmentation of brain stroke image.	Abdulrahman, A.	This study used binary method which uses pixels to decide if the patient has the disease or not and morphological operation which uses erosion and dilation. However, both methods do not show any maturity of the disease by providing accuracy percentage and confusion matrix which may help in interpreting the images, therefore, both methods don't outperform human beings since they don't provide more information about the disease [9].

Table 3.1 Summary of related works and gaps

**3.8 Conclusion**

The following are the methods used in this chapter's overview of the pertinent literature and methods for detecting cerebrovascular illness using MRI images: automatic cerebrovascular diagnosis frequently employs picture methods based on object classification, customised feature methods, and the DT, a supervised classifier that has been applied in various studies to identify brain disorders. methods based on segmenting objects in images with semantics are employed for cerebral vascular segmentation. Cerebrovascular disease detection utilizing medical pictures and AI models is still a difficult task, and For this disease identification to be more accurate, more research is needed. In light of this, the process for implementing a detection model that may help in enhancing the accuracy when identifying cerebrovascular disease is discussed in the following chapter.

## **CHAPTER 4: METHODOLOGY**

### **4.1 Introduction**

The basic structure of this chapter presents the four essential stages of our proposed method as follows: segmentation, feature extraction, CNN creation, and detection. The MRI scans were provided to the CNN model to enable image detection and generate the accuracy rate and confusion matrix. In addition, the tools and processes utilized to implement the suggested system, namely, detection of cerebrovascular disease in brain images using CNN are covered in this chapter.

### **4.2 Dataset**

Brain images using MRI was obtained from Kaggle publicly available dataset. Turfloop Research Ethics Committee (TREC) confirmed that the study involves secondary use of data and has no ethical implication. After they reviewed the study protocol, the TREC granted the researcher permission to proceed with the research. The dataset was divided into two folders, infected and not infected images. Infected images are represented by Yes while not infected is represented by No. The total number of infected images is 155 while not infected images is 98. The following figure 4.1 illustrate the two folders of infected and not infected MRI Scans.

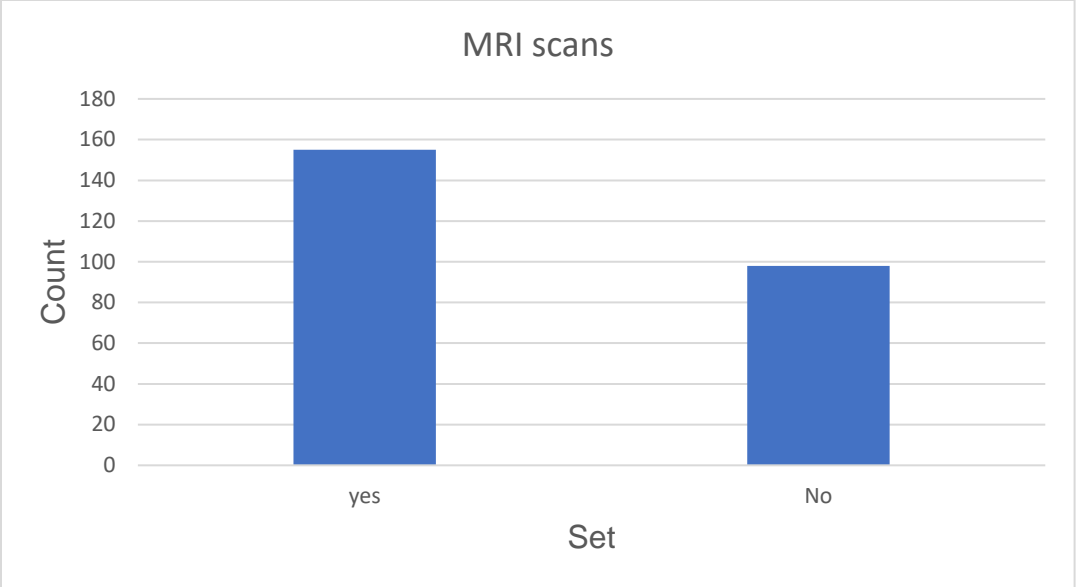


Figure 4.1 MRI scans

The dataset was split into three subfolders, namely, training, validation and testing using python library called sklearn. Sklearn is a python library that is mostly used to separates the dataset in machine learning tasks [50]. Training subfolder contains 119 infected images and 74 not infected images, validation subfolder contains 31 infected images and 19 not infected images and testing subfolder contains 5 infected images and 5 not infected images as illustrated in figure 4.2

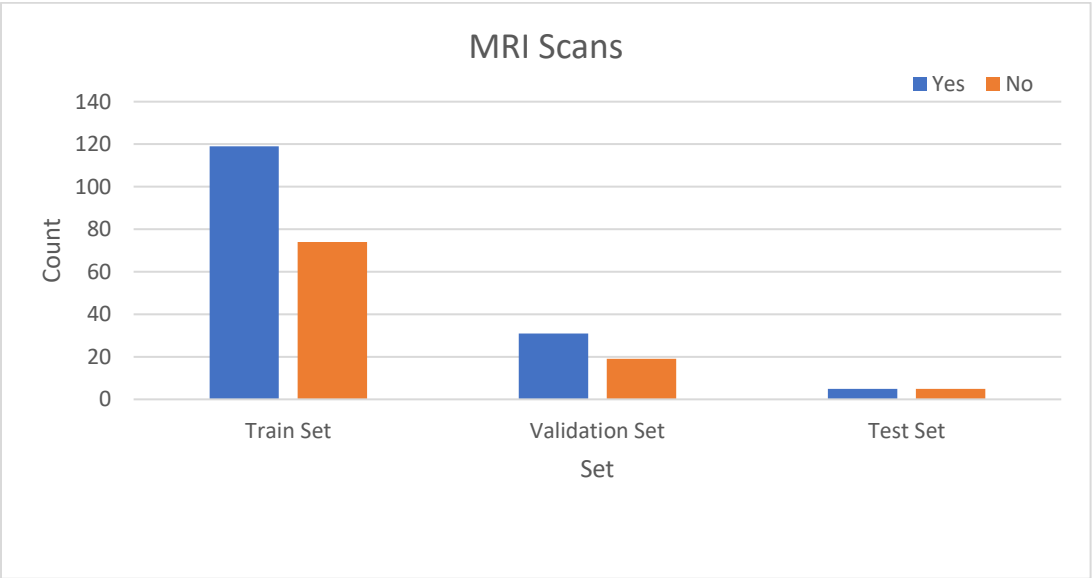


Figure 4.2 splitting of data

The datasets contains images of different width and height. Figure 4.3 below shows the histogram of ratio distributions to illustrate the difference in width and height of the dataset.

```
plt.hist(RATIO_LIST)
plt.title('Distribution of Image Ratios')
plt.xlabel('Ratio Value')
plt.ylabel('Count')
plt.show()
```

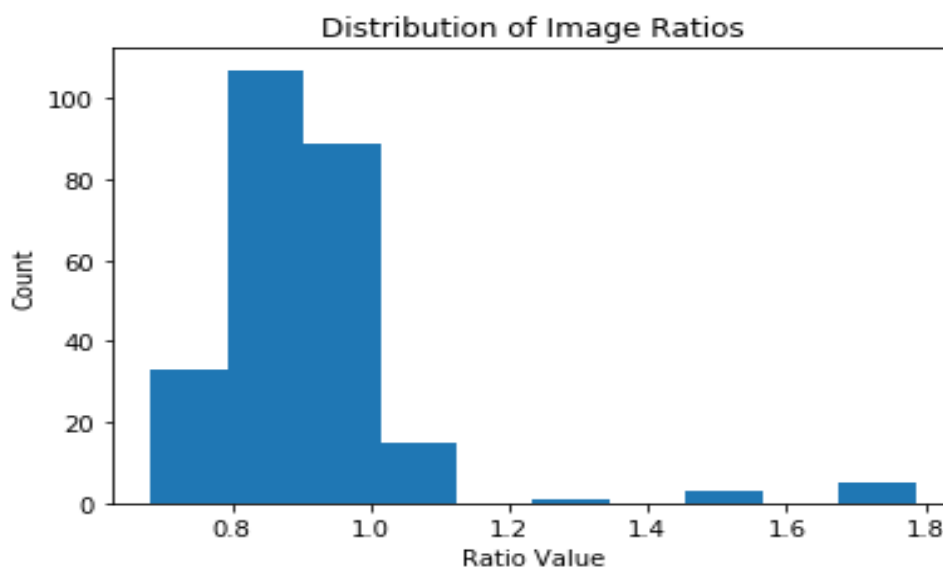


Figure 4.3 Distribution of image ratios

### 4.3 Implementation Tools

Detection of cerebrovascular disease in brain images using CNN was implemented on Jupyter notebook using python computer vision in windows 10 operating system. Python is a programming language that aims to make it easy for programmers of all skill levels to translate their ideas into working code. Many developers utilize Python since it is the

most well-known, established, and supported programming language for machine learning, that is why it is often featured in CVs. Contrarily, computer vision enables computers to identify objects in digital stills or moving pictures [29]. Python allows developers to automate procedures that call for visualization. Python libraries that were created to aid data scientists, particularly when it comes to data processing, modeling, and data visualization, as well as their excellent functionality to deal with mathematics, statistics, and scientific function, were major factor in the study's decision to use Python for computer vision [51]. Figure 4.4 shows the python libraries that were used in this study:

```
import numpy as np
from tqdm import tqdm
import cv2
import os
import shutil
import itertools
import imutils
import matplotlib.pyplot as plt
from sklearn.preprocessing import LabelBinarizer
from sklearn.model_selection import train_test_split
from sklearn.metrics import accuracy_score, confusion_matrix

import plotly.graph_objs as go
from plotly.offline import init_notebook_mode, iplot
from plotly import tools

from keras.preprocessing.image import ImageDataGenerator
from keras.applications.vgg16 import VGG16, preprocess_input
from keras import layers
from keras.models import Model, Sequential
```

Figure 4.4 python libraries

### I. NumPy

Array manipulation is done using the NumPy Python library. Numerical Python is known as NumPy. It also offers functions for working in the field of linear algebra as well as matrices and the Fourier transform. Travis Oliphant created NumPy in the year 2005. It is open source and available for free [51].

### II. Tqdm



The Arabic term for progress, taqaddum, is the root of the word tqdm. It is used to create progress meters and progress bars, Python's tqdm library is utilized. We can easily implement tqdm in our loops, functions, and even Pandas [40].

### III. Cv2

It is a free library that may be used to carry out operations like disease detection, face recognition, object tracking, landmark recognition, and many other things. CV2 is an acronym for computer vision [50].

### IV. Os

The Python OS module gives users the ability to create interactions with their operating systems. It provides a variety of practical OS features that may be utilized to carry out OS-based tasks and obtain pertinent OS-related data. Python's basic utility modules cover the OS [42].

### V. Shutil

In the Python language, the shutil module provides a number of functions for dealing with operations on files and associated collections. It gives users the option to copy and delete files. It resembles the OS Module in certain ways, but the OS Module does contain features that deal with file collections [40].

### VI. Itertools

Itertool is a package in Python that offers a number of operations on iterators to create complicated iterators. Iterator algebra can be created quickly and efficiently with the help of this module [50].

### VII. Imutils

Imutils is a straightforward Python image processing toolkit that may be used to translate, rotate, resize, skeletonize, or calculate the blur intensity in an image. Imutils will look for functions in those packages as well if NumPy, SciPy, Matplotlib, and OpenCV are already installed[51].

### VIII. Matplotlib

Python Matplotlib is a cross-platform package for graphical data visualization and charting. Developers can incorporate plots into GUI systems by using the matplotlib application programming interfaces [51].

IX. Sklearn

Python's Sklearn library is used for machine learning. It's a collection of effective tools for data mining and analysis, to be more precise. The framework is constructed on top of a number of well-known Python programs, including Matplotlib, SciPy, and NumPy [50].

X. Plotly

An interactive, open-source plotting toolkit for Python, Plotly offers more than 40 different chart types for a range of statistical, financial, geographic, scientific, and three-dimensional use-cases[51].

XI. keras

Keras is an open source Python library that is free and powerful for building and analyzing deep learning models. With just a few lines of code, it is a component of the TensorFlow library and enables users to construct and train neural network models[42].

#### 4.4 Overall Workflow of the Proposed System

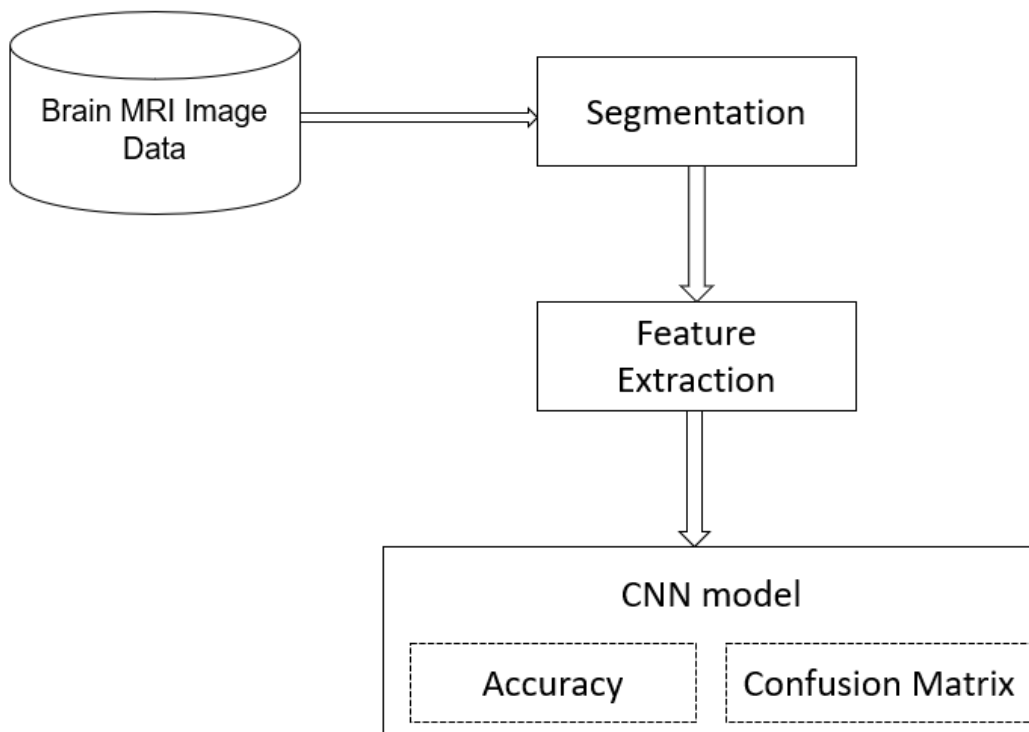


Figure 4.5 Diagram of the proposed system

##### 4.4.1 Segmentation

This section answered the first research question, how will brain cropping process from brain images be automated.

It is an approach of image segmentation, which is frequently used in digital image processing and analysis to split an image into a number of sections or areas based on the properties of the pixels in the picture [40]. There are several different kinds of artifacts that might appear in brain images, a non-homogeneous intensity range, for instance, different size of images in the dataset. segmentation is a method that has been developed to remove the artifacts and resize images to a fixed size to lessen the deformation [40]. Brain images using MRI were obtained from Kaggle publicly available dataset which contains different sizes of images. As a result of this non-homogeneity, namely, different

sizes of images in the dataset, there will be high deformation of features and patterns if the CNN model were to be fitted using this dataset and also the results accuracy will be degraded due to deformation [50]. In this study segmentation was used to resize the images since the dataset contains images of different sizes which can influence results accuracy erroneously by producing misleading results such as false positives and false negatives.

#### **4.4.2 Feature Extraction**

In the CNN procedure, the CNN approach is employed for feature extraction because it is currently the go-to model on any image-related problem. The feature extraction process extracts feature from the segmented brain. At the start of the network, basic visual attributes including edges, corners, and blobs are recorded. Higher level picture features are then created by analyzing these fundamental qualities using deeper network layers. These more stringent standards are preferred for categorizing cerebrovascular disease because they take into account all the basic characteristics and produce a clearer picture. Given the abundance of scores that match the relevant detection labels, such as background and normal brain, the layer immediately beneath the detection layer is typically an effective location for feature extraction. Each pixel in the MRI pictures is converted into a four-dimensional feature vector with values that are equivalent to the feature extraction layer's probability values [41].

#### **4.4.3 CNN Model**

This section answered the second research question, How will CNN model be implemented.

In this section, figure 4.5 shows the CNN architecture that was used in this study with its building blocks. CNNs are a subset of artificial neural networks that have gained a reputation for being extremely effective at both image categorization and detection. A CNN's building blocks include convolution layers, pooling layers and fully connected layers. The model's performance was evaluated by its accuracy rate and confusion matrix.

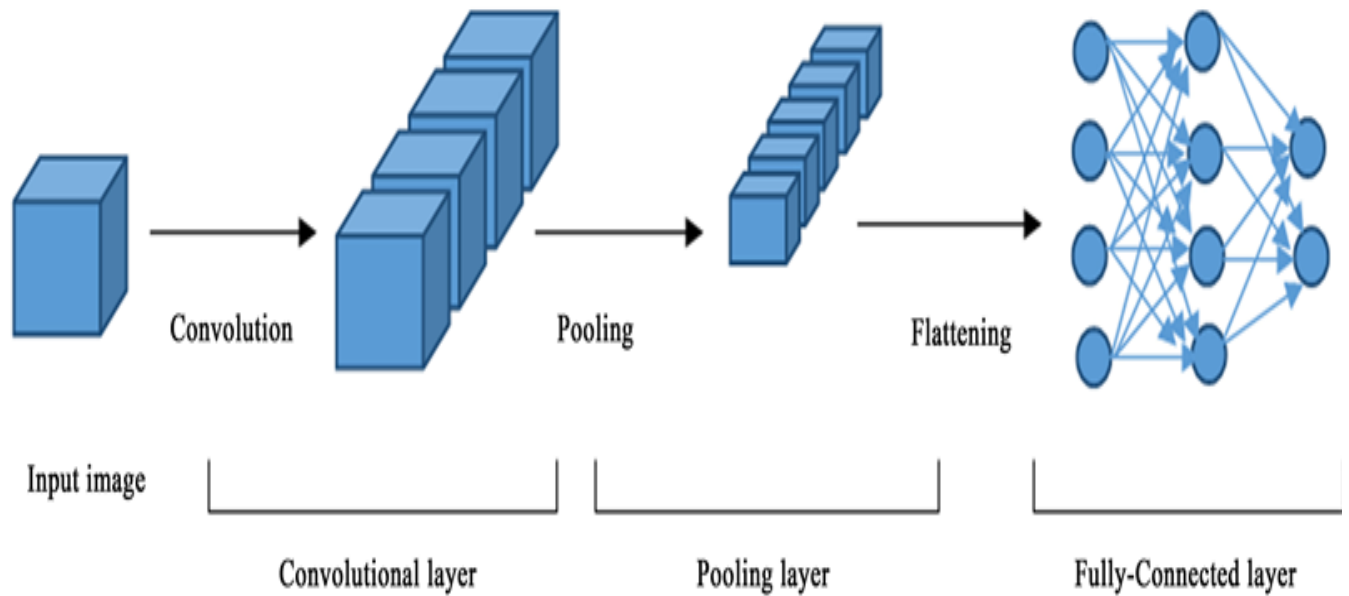


Figure 4.6 CNN architecture

### I. Convolution Layer

The foundation of a CNN is a convolutional layer. It has several filters or kernels, the settings of which must be memorized throughout training. The size of the filters is typically smaller than the original image. Each filter produces an activation map after it convolves with the image. In its receptive area, a convolution combines all the pixels into a single value. Applying a convolution, for instance, to an image would result in both a reduction in image size and the condensing of all field data into a single pixel. The convolutional layer's final output is a vector [42].

### II. Pooling Layers

By pooling layers, the feature map size is decreased. Therefore, it requires fewer parameters to be learned and requires less network processing. The features that are present in a specific area are summarized in the feature map produced by the feature pooling layer of a convolution layer [54].

### III. Fully Connected Layer

The Fully Connected Layer is made up of forward-feeding neural networks. Fully Connected Tiers refer to the network's uppermost layers. The last convolutional or pooling layer's output is sent to the fully connected layer, where it is flattened before being used [56].

#### **4.4.3.1 Accuracy**

This section answered the last research question, how will CNN model be tested to see if it produces accurate results.

Accuracy was used to assess just how well the average measurement of multiple measurements stacks up against the standard measurement of the same item or the true value. Accuracy is measured as the proportion of correctly predicted images in the test set, compared to all the images in the same test set. It is defined by the following equation:

$$\text{Accuracy} = \frac{\text{Number of correctly predicted images}}{\text{Total number of tested images}}$$

The Receiver Operating Characteristics (ROC) curve was used to plot the performance of accuracy rate.

#### **4.4.3.2 Confusion Matrix**

In machine learning, an evaluation of a classification algorithm's performance is done using a table called a confusion matrix. The effectiveness of a classification algorithm is displayed and summarized via a confusion matrix. The performance of a trained model is determined by how good the predictions reflect the actual classes. The evaluation measurements are given in the following terms:

- I. FP = False positive means observations where the actual class is negative, and the predicted class is positive.
- II. TN = True negative means observations where the actual and predicted class is negative.

- III. TP = True positive means observations where the actual and predicted class is positive.
- IV. FN = False negative means observations where the actual class is positive, and the predicted class is negative.

Confusion Matrix			
Model Class		Actual Class	
		Positive	Negative
Predicted class	Positive	True Positive	False Positive
	Negative	False Negative	True Negative

Table 4.1 Confusion Matrix

#### 4.5 Conclusion

This chapter has discussed the four main stages of our suggested method namely: segmentation, feature extraction, CNN design and detection. In the segmentation step, the MRI images were resized, The MRI images were then fed to CNN model to detect images and produce the accuracy rate and confusion matrix. This chapter also discussed the dataset, implementation tools and procedures used to implement the proposed system.

#### 4.6 Summary

Brain images using MRI was obtained from Kaggle publicly available dataset. The dataset was divided into two folders, infected and not infected images. The CNN model was implemented using python programming language due to its libraries that were created to aid data scientists, particularly when it comes to data processing, modelling, and data visualization. Segmentation was used to resize the images since the dataset contains images of different sizes which can influence results accuracy erroneously by producing misleading results such as false positives and false negatives. A CNN's building blocks

are convolution layers, pooling layers and fully connected layers. The model's performance was evaluated by its accuracy rate and confusion matrix.



## CHAPTER 5: RESULTS

### 5.1 Introduction

This chapter describes the implementation and evaluation of results of CNN model for detection of cerebrovascular disease in the brain. The segmentation methods, the parameter settings of the model and the results analysis are described. The Receiver Operating Characteristics (ROC) curve was used to plot the performance of accuracy rate of the model and confusion matrix was also used to measure the performance of the CNN model.

### 5.2 Segmentation

This section answered the first research objective, Automate the process of brain cropping from brain images.

Digital image processing and analysis frequently employ the technique of segmentation, which is frequently based on the characteristics of the pixels in the image [40]. Segmentation divides an image into various parts or areas. In this study segmentation was used to resize the images with different width and height as shown in figure 5.1. Fitting the CNN model with images of different sizes may cause high deformation of features and patterns which may affect accuracy of the results. We applied the segmentation steps below to all the images in the dataset to resize the images to a fixed size to lessen the probability of deformation:

- I. Crop the image's most crucial portions.
- II. To resize the images to have an equal width and height
- III. Use normalization to bring pixel values within the 0 and 1 range.

Figure 5.1 to figure 5.4 below shows the steps that were followed when resizing the images.

```
plt.subplot(141)
plt.imshow(img)
plt.xticks([])
plt.yticks([])
plt.title('Step 1. Get the original image')
plt.subplot(142)
plt.imshow(img_cnt)
plt.xticks([])
plt.yticks([])
plt.title('Step 2. Find the biggest contour')
plt.subplot(143)
plt.imshow(img_pnt)
plt.xticks([])
plt.yticks([])
plt.title('Step 3. Find the extreme points')
plt.subplot(144)
plt.imshow(new_img)
plt.xticks([])
plt.yticks([])
plt.title('Step 4. Crop the image')
plt.show()
```

Firstly, one image was chosen to illustrate how the segmentation of resizing an image is done. The image was imported from the dataset as shown in figure 5.1 below.

Step1 The original image from the dataset

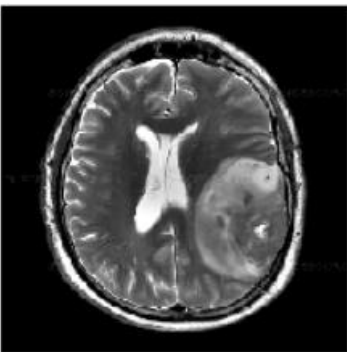


Figure 5.1 original image

The second step is to segment the image. This process was computed using the convex hull of the brain. A binary image's convex hull is the collection of pixels included in the

smallest convex polygon that encircles every white pixel in the input [50] and is outlined in aqua color in figure 5.2 below.

Step 2. Find the biggest contour

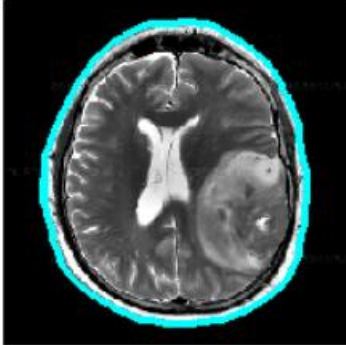


Figure 5.2 biggest contour

The third step is to find the coordinates of the extreme points on the contour. Contour is the line connecting all the points along an image's edge that have the same intensity [58]. For the purposes of object detection, estimating the size of a target object, and form analysis, contours are helpful, which are the x-coordinates (west and east) and the y-coordinates (north and south), after, a circle was drawn for each extreme points as detailed below:

X- coordinates: West=blue and East= green

Y-coordinates: North=red and South=yellow

As shown by figure 5.3 below.

Step 3. Find the extreme points

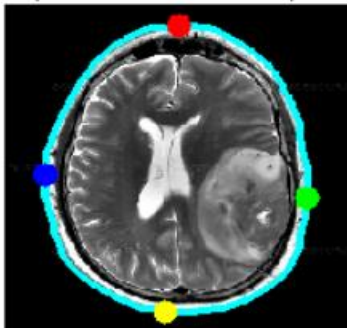


Figure 5.3 extreme points

The final step is to use the thresholding method to segment the brain from the rest of the image. Thresholding is a method used to convert a full-color or grayscale image into a binary image [40]. In order to facilitate image processing, this is frequently done to segregate an object or foreground pixels from background pixels. The study computed the thresholding method by cropping the images to size 240 width and 240 height because the more pixels per inch, the finer the detail on the image and larger the fixed size of images, the less shrinking required. Less shrinkage results in less distortion of the image's internal characteristics and patterns. This will lessen the deterioration of classification accuracy brought on by deformations. figure 5.4 below shows the cropped image.

Step 4. Crop the image

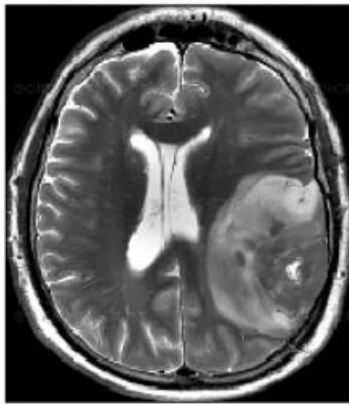


Figure 5.4 cropped image

50 images from the yes folder which contains the MRI images that are infected by cerebrovascular disease and no folder which contains images that are not infected by cerebrovascular disease were chosen by the researcher to show the results of the segmentation method. Figure 5.5 show 50 images which are infected by cerebrovascular disease and figure 5.6 show 50 images which are not infected by cerebrovascular disease.

```

def plot_sample_images(X, y, n=50):
    """
    Plots n sample images for both values of y (labels).
    Arguments:
        X: A numpy array with shape = (#_examples, image_width, image_height, #_channels)
        y: A numpy array with shape = (#_examples, 1)
    """

    for label in [0,1]:
        # grab the first n images with the corresponding y values equal to label
        images = X[np.argwhere(y == label)]
        n_images = images[:n]

        columns_n = 10
        rows_n = int(n/ columns_n)

        plt.figure(figsize=(20, 10))

        i = 1 # current plot
        for image in n_images:
            plt.subplot(rows_n, columns_n, i)
            plt.imshow(image[0])

            # remove ticks
            plt.tick_params(axis='both', which='both',
                            top=False, bottom=False, left=False, right=False,
                            labelbottom=False, labeltop=False, labelleft=False, labelright=False)

            i += 1

        label_to_str = lambda label: "Yes" if label == 1 else "No"
        plt.suptitle(f"cerebrovascular disease: {label_to_str(label)}")
        plt.show()

```

```
plot_sample_images(X, y)
```

Images that are infected by cerebrovascular disease have the presence of blood clot on the image of the brain as shown below.

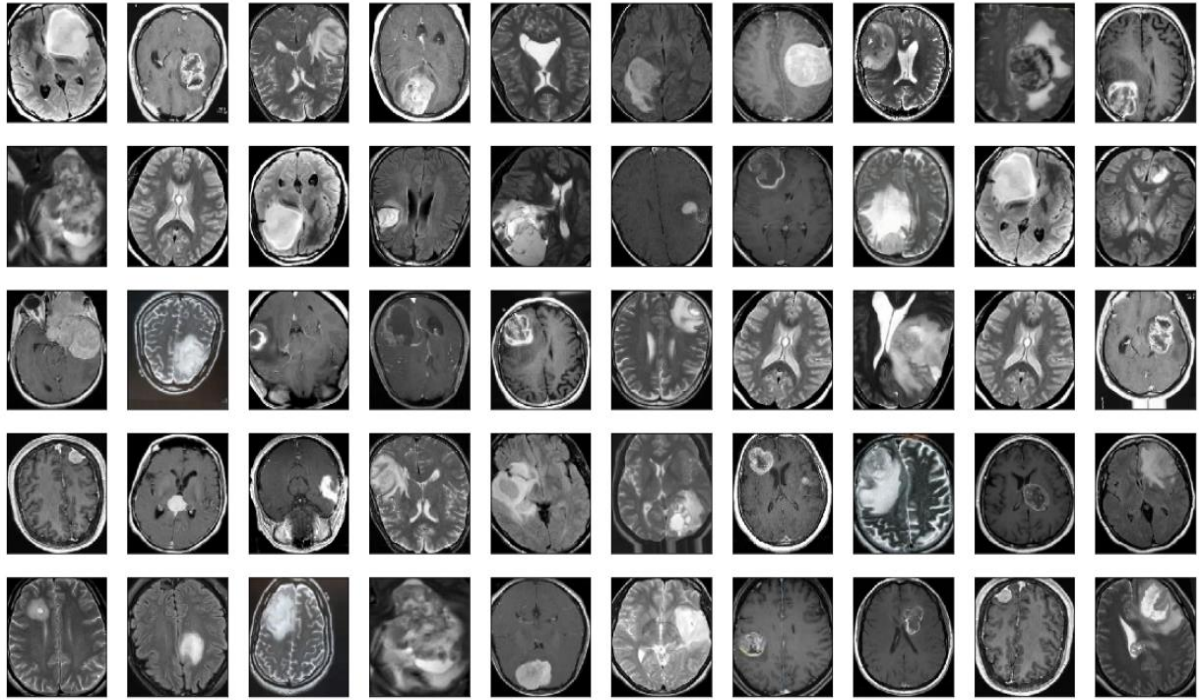


Figure 5.5 Images infected by cerebrovascular disease

Images that are not infected by cerebrovascular disease don't have blood clot on the image of the brain as shown below.

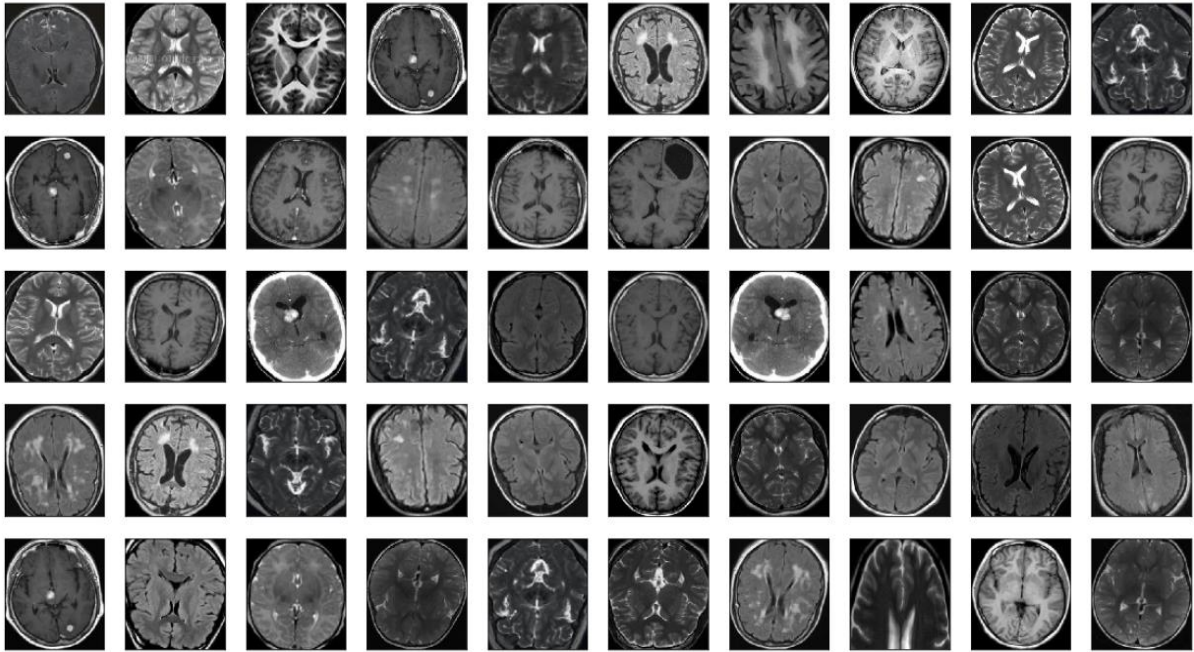


Figure 5.6 Images not infected by cerebrovascular disease

## 5.4 CNN Model

This section answered the second and the last research objectives, Implement CNN to detect any abnormalities from brain images and to test the CNN model to see if it produces accurate results.

CNNs are a subset of deep learning methods that have been popular in a variety of computer vision applications and are drawing interest from a wide range of industries, including radiology. Convolution layers, pooling layers, and fully connected layers are just a few of the building pieces that CNN employs to automatically and adaptively learn spatial feature hierarchies through backpropagation. This section explains the source code and the results that were found while building the CNN detection model of cerebrovascular disease.

```
def build_model(input_shape):
    """
    Arguments:
        input_shape: A tuple representing the shape of the input of the model. shape=(image_width, image_height, #_cha
    Returns:
        model: A Model object.
    """
    # Define the input placeholder as a tensor with shape input_shape.
    X_input = Input(input_shape) # shape=(?, 240, 240, 3)

    # Zero-Padding: pads the border of X_input with zeroes
    X = ZeroPadding2D((2, 2))(X_input) # shape=(?, 244, 244, 3)

    # CONV -> BN -> RELU Block applied to X
    X = Conv2D(32, (7, 7), strides = (1, 1), name = 'conv0')(X)
    X = BatchNormalization(axis = 3, name = 'bn0')(X)
    X = Activation('relu')(X) # shape=(?, 238, 238, 32)

    # MAXPOOL
    X = MaxPooling2D((4, 4), name='max_pool0')(X) # shape=(?, 59, 59, 32)

    # MAXPOOL
    X = MaxPooling2D((4, 4), name='max_pool1')(X) # shape=(?, 14, 14, 32)

    # FLATTEN X
    X = Flatten()(X) # shape=(?, 6272)
    # FULLYCONNECTED
    X = Dense(1, activation='sigmoid', name='fc')(X) # shape=(?, 1)

    # Create model. This creates your Keras model instance, you'll use this instance to train/test the model.
    model = Model(inputs = X_input, outputs = X, name='BrainDetectionModel')

    return model
```

Figure 5.7 building the model

Figure 5.7 illustrate the source code that was used to build the CNN model. The input shape that was fed to CNN model is as follows, image width (240), image height (240) and there are stored as (240,240,3) they are used to extract neighbouring pixels. CNN

model had convolutional layer with a spatial filter of 32. A max pooling layer with a pool size of (4x4), came after the convolutional layers.

```

IMG_SHAPE = (IMG_WIDTH, IMG_HEIGHT, 3)

model = build_model(IMG_SHAPE)

model.summary()

```

Layer (type)	Output Shape	Param #
input_1 (InputLayer)	(None, 240, 240, 3)	0
zero_padding2d (ZeroPadding2D)	(None, 244, 244, 3)	0
conv0 (Conv2D)	(None, 238, 238, 32)	4736
bn0 (BatchNormalization)	(None, 238, 238, 32)	128
activation (Activation)	(None, 238, 238, 32)	0
max_pool0 (MaxPooling2D)	(None, 59, 59, 32)	0
max_pool1 (MaxPooling2D)	(None, 14, 14, 32)	0
flatten (Flatten)	(None, 6272)	0
fc (Dense)	(None, 1)	6273

```

Total params: 11,137
Trainable params: 11,073
Non-trainable params: 64

```

Figure 5.8 output of the CNN model

The output of every Convolution layer of 2 Dimensional (Conv2D) and height dimensions tend to decrease as you get deeper into the network, as shown above. The first option regulates how many output channels each Conv2D layer has. Typically, we can afford (computationally) to add more output channels in each Conv2D layer as the width and



height decrease. The network summary reveals that before passing through one Dense layer, the outputs of (14, 14, 32) were flattened into vectors of shape (6273).

```
EPOCHS = 30
es = EarlyStopping(
    monitor='val_acc',
    mode='max',
    patience=6
)

history = model.fit_generator(
    train_generator,
    steps_per_epoch=50,
    epochs=EPOCHS,
    validation_data=validation_generator,
    validation_steps=25,
    callbacks=[es]
)
```

Figure 5.9 Epochs

Figure 5.9 shows the number of batches of data from our training and validating set that should be supplied to the model before announcing the completion of an epoch which for training is 50 steps per epoch and for validating is 25 since dataset in training is not equal to the dataset in validation subfolder, and 30 batches will cover the whole training and validation dataset.

```

Epoch 1/30
50/50 [=====] - 26s 518ms/step - loss: 3.0781 - acc: 0.6049 - val_
loss: 2.2196 - val_acc: 0.7563
Epoch 2/30
50/50 [=====] - 24s 476ms/step - loss: 2.2948 - acc: 0.7411 - val_
loss: 2.0424 - val_acc: 0.8006
Epoch 3/30
50/50 [=====] - 23s 465ms/step - loss: 2.1530 - acc: 0.7635 - val_
loss: 1.9332 - val_acc: 0.8418
Epoch 4/30
50/50 [=====] - 23s 468ms/step - loss: 1.9035 - acc: 0.7910 - val_
loss: 1.5734 - val_acc: 0.8609
Epoch 5/30
50/50 [=====] - 24s 471ms/step - loss: 2.0054 - acc: 0.7719 - val_
loss: 1.2197 - val_acc: 0.8418
Epoch 6/30
50/50 [=====] - 23s 466ms/step - loss: 1.6505 - acc: 0.8236 - val_
loss: 1.1466 - val_acc: 0.8829
Epoch 7/30

```

Figure 5.10 training epoch

Our output in figure 5.10 shows that this model performed admirably on the training set, with accuracy exceeding 80% and loss coming very close to zero.

```

plt.subplot(1, 2, 1)
plt.plot(epochs_range, acc, label='Train Set')
plt.plot(epochs_range, val_acc, label='Val Set')
plt.legend(loc="best")
plt.xlabel('Epochs')
plt.ylabel('Accuracy')
plt.title('Model Accuracy')

plt.subplot(1, 2, 2)
plt.plot(epochs_range, loss, label='Train Set')
plt.plot(epochs_range, val_loss, label='Val Set')
plt.legend(loc="best")
plt.xlabel('Epochs')
plt.ylabel('Loss')
plt.title('Model Loss')

plt.tight_layout()
plt.show()

```

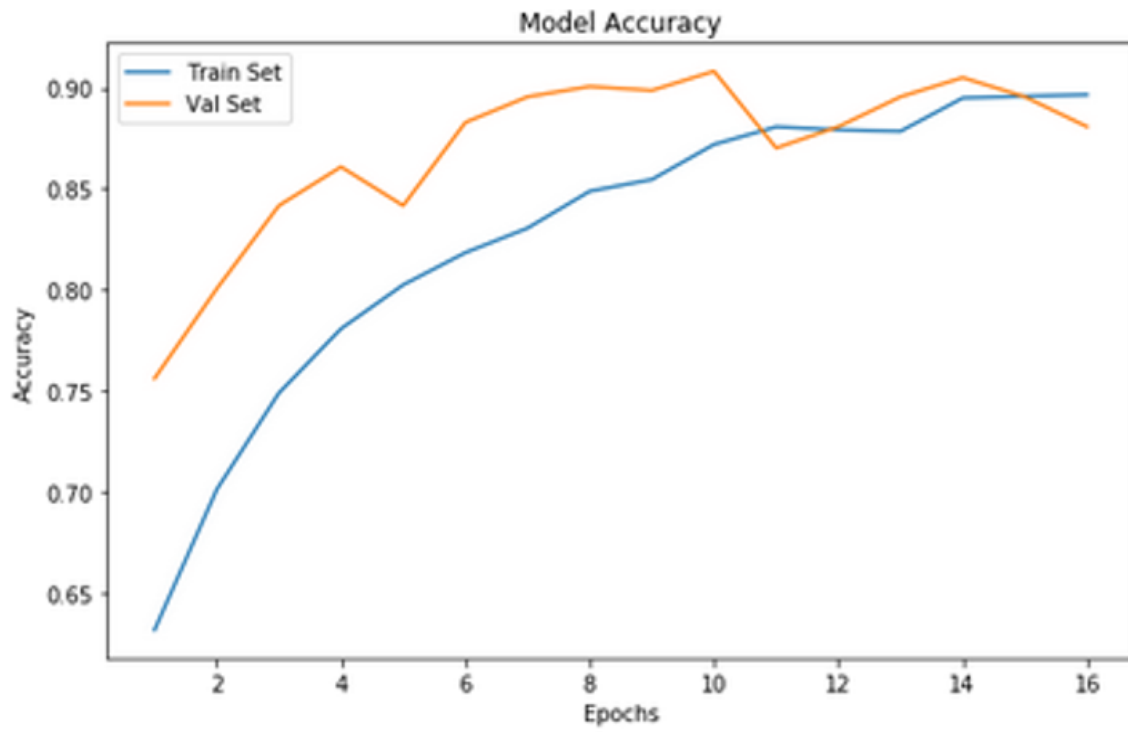


Figure 5.11 accuracy model

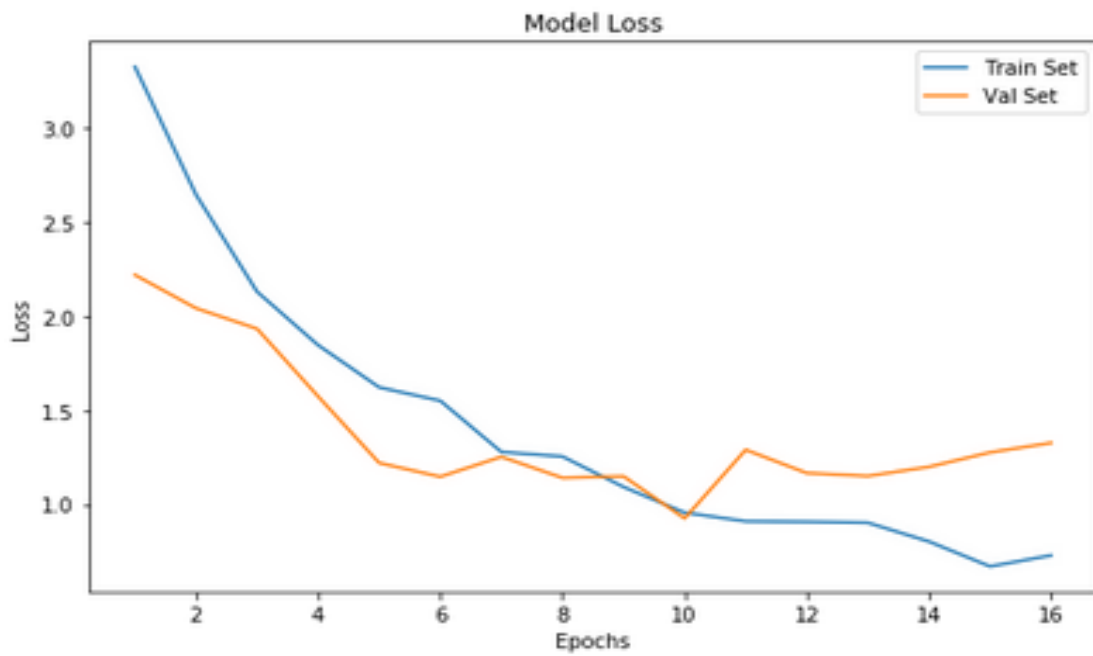


Figure 5.12 model loss

Figure 5.11 and Figure 5.12 above displays the accuracy and loss of the CNN model on the training and validation dataset. The plot above is based on 16 epochs since the model was trained using `model.Fit()` function, this made the history to only contain the metric values of the first 16 epochs. The model was trained over 30 iterations, and the study determined the accuracy of training and validation considering the binary problem, the loss of training and validation considering the binary problem, and the accuracy of training and validation considering the multiclass problem, as well. Each curve that is presented is derived from the history of the Keras model, which computes accuracy and loss for each epoch that the network completes. By contrasting the anticipated class with the actual class, accuracy is determined. The cross-entropy value between the predicted class and the actual class is used to calculate loss.

```
# validate on val set
predictions = model.predict(X_val_prep)
predictions = [1 if x>0.5 else 0 for x in predictions]

accuracy = accuracy_score(y_val, predictions)
print('Val Accuracy = %.2f' % accuracy)

confusion_mtx = confusion_matrix(y_val, predictions)
cm = plot_confusion_matrix(confusion_mtx, classes = list(labels.items()), normalize=False)
```

```
Val Accuracy = 0.90
```

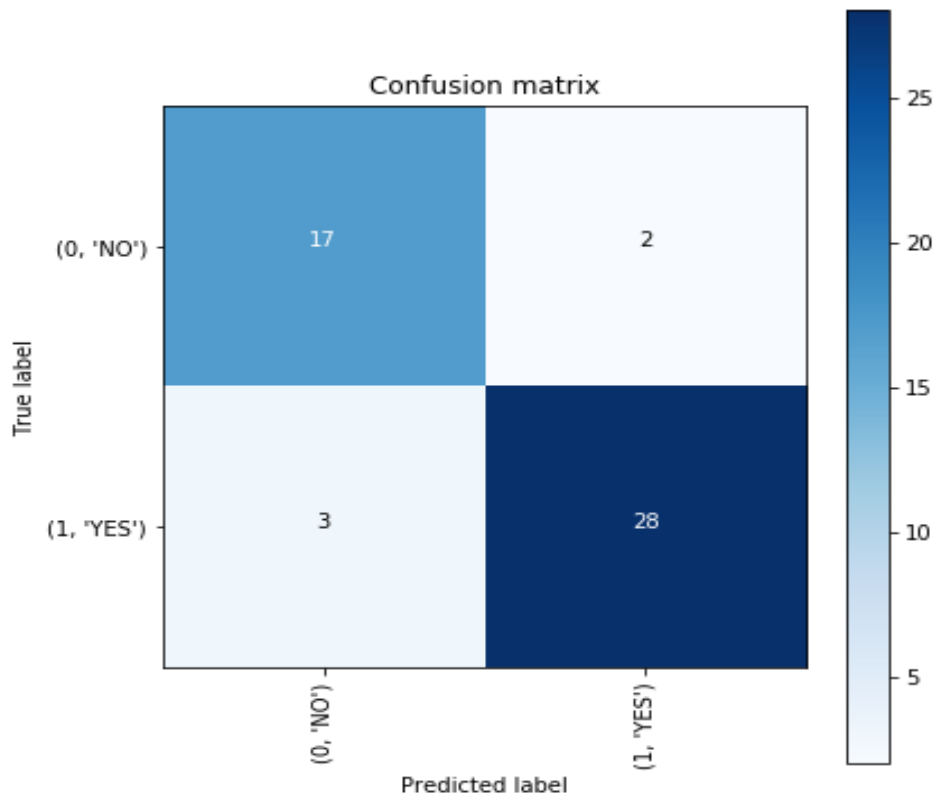


Figure 5.13 confusion matrix for validation accuracy

The confusion matrix in figure 5.13 was based on 30 images in the validation dataset folder. The results are as follows: 17 were true positively detected, 2 were false positively detected, 3 were false negatively detected and 28 were true negatively detected. The designed CNN model has a validation accuracy rate of 90%.

```
# validate on test set
predictions = model.predict(X_test_prep)
predictions = [1 if x>0.5 else 0 for x in predictions]

accuracy = accuracy_score(y_test, predictions)
print('Test Accuracy = %.2f' % accuracy)

confusion_mtx = confusion_matrix(y_test, predictions)
cm = plot_confusion_matrix(confusion_mtx, classes = list(labels.items()), normalize=False)

Test Accuracy = 0.80
```

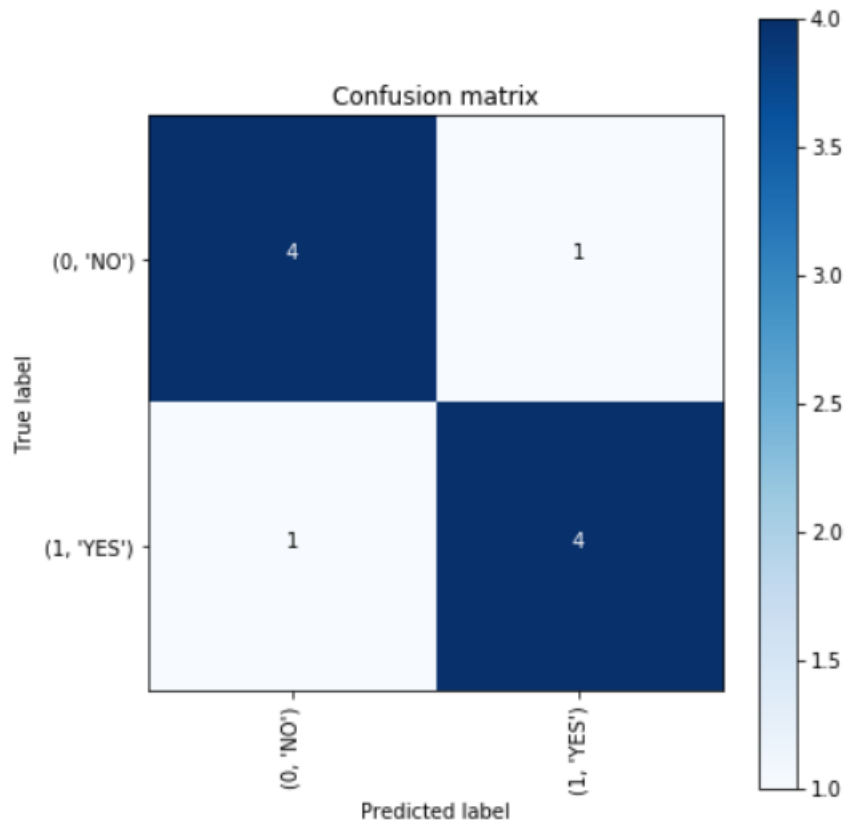


Figure 5.14 confusion matrix for test accuracy

The confusion matrix in figure 5.14 shows that 4 out of 5 images in the test dataset folder were correctly detected (true positive and true negative) and 1 out of 5 images was incorrectly detected (false positive and true negative). The designed CNN model has a test accuracy rate of 80%.

## 5.5 Discussion

This study trained, validated, and tested the CNN model for detecting cerebrovascular illness using publicly available data from Kaggle. However, the dataset came with images of different sizes, therefore, the dataset was resized to 240\*240 pixels to avoid high deformation of features and patterns. The input shape that was fed to CNN model was as follows, image width(240), image height(240) and there are inputted as(240,240,3) they are used to extract neighbouring pixels. CNN model had convolutional layer with a spatial filters of 32. A max pooling layer with a pool size of (4x4) came after the convolutional layers. The 3-dimensional matrix was flattened into a 1-dimensional vector as a result of

the CNN model's output, called flatten layer. Subsequently, a dense fully connected layer with one neuron with a sigmoid activation since this is a binary detection task.

The evaluation results show that the CNN model detect cerebrovascular disease successfully with validation accuracy rate of 90% and test accuracy rate of 80%. The results were illustrated on ROC and confusion matrix. The existing studies on cerebrovascular disease detection used binary method which uses pixels to decide if the patient has the disease or not and they also used morphological operation which uses erosion and dilation, However, both studies do not outperform this study since their methods do not show accuracy rate and confusion matrix which may help in interpreting the images. This also showed that the CNN model implemented in this study can detect cerebrovascular disease successfully, but when we compare our findings to other studies that used CNN to detect diseases like pneumonia and breast cancer, the results of pneumonia were 95% accurate and the results of breast cancer were 92% accurate, so our study needs to be improved since we got 80% accuracy rate from the test dataset.

## **5.6 Conclusion**

segmentation was used to resize the images since the dataset came with images of different sizes which could have influenced the results accuracy erroneously by producing misleading results such as false positives and false negatives. The CNN model was used to predict whether the MRI images have cerebrovascular disease or not. The model have successfully detected the images with a validation accuracy rate of 90% and test accuracy rate of 80%. This study outperforms existing studies on cerebrovascular disease detection since this study shows accuracy rate and confusion matrix.

## **5.7 Summary**

The dataset was resized to equal width and height of 240 using the segmentation process. The input shape that was fed to CNN model was as follows, image width (240), image height(240) and there were inputted as(240,240,3), they are used to extract neighbouring pixels. The evaluation results show that the CNN model detect cerebrovascular disease successfully with validation accuracy rate of 90% and test accuracy rate of 80%.

The results were illustrated on ROC and confusion matrix. This also showed that the CNN model implemented in this study can detect cerebrovascular disease successfully.



## **CHAPTER 6: CONCLUSION**

### **6.1 Introduction**

Our study focused on detecting cerebrovascular disease using CNN model. This section summarizes the study's findings and offers suggestions for additional research that builds on the previous work. Presenting gaps in the current study may be accomplished by including a section on future research.

### **6.2 Research Summary**

The aim of the study was to detect cerebrovascular disease from brain images using CNN as indicated in chapter 1. We wanted to develop a CNN model that will produce accuracy rate and also show the confusion matrix which may help radiologists in interpreting the images. Detection of cerebrovascular disease from brain images using CNN was implemented on Jupyter notebook using python computer vision in windows 10 operating system and MRI brain scans were collected from the Kaggle public dataset.

The first objective was to automate the process of brain cropping from brain images, we did this by using segmentation method since the dataset came with images of different sizes which could have influenced the results accuracy erroneously by producing misleading results such as false positives and false negatives. The first step was to import the original image from the dataset, the second step was to segment the image using convex hull process to collect the pixels included in the smallest convex polygon that encircles every white pixels in the input, the third step was to find the coordinates of the extreme points on the contour and the last step was to use the thresholding method to segment the brain from the rest of the image. This objective was achieved because we managed to resize all the images in the dataset to a width and height of 240.

The second objective was to implement CNN model to detect any abnormalities from the brain images, we did this by using a number of building blocks, such as convolution layers, pooling layers, and fully connected layers, to develop a CNN model that would automatically and adaptively learn spatial hierarchies of feature through backpropagation.

Image width (240), image height (240), and number of channels (3) are the input shapes that were fed to the CNN model and they are utilized to extract nearby pixels. Convolutional layer with 32 spatial filters. A max pooling layer with a pool size of (4 x4), came after the convolutional layers. The output of the CNN model, flatten layer, flattened the 3-dimensional matrix into a 1-dimensional vector. A dense fully connected layer with one neuron with sigmoid activation is utilized because this is a binary detection challenge. This objective was achieved because the CNN model that was implemented managed to detect abnormalities and produced accuracy rate and confusion matrix.

The third objective was to test the CNN model to see if it produces accurate results, we tested the model using images from the test dataset. The evaluation results shown that the CNN model detected cerebrovascular disease successfully with a test accuracy rate of 80%. The confusion matrix shown that 4 out of 5 images in the test dataset folder were correctly detected(true positive and true negative) and 1 out of 5 images was incorrectly detected (false positive and true negative). This objective was achieved because the CNN model produced accuracy rate and confusion matrix.

The results were illustrated on ROC and confusion matrix. CNN model implemented in this study can detect cerebrovascular disease successfully, however, when we compare our results to other studies that used CNN to detect diseases such as pneumonia and breast cancer detection, the results of pneumonia was 95% accurate and breast cancer was 92% accurate, therefore, which means our study need to be improved since we got 80% accuracy rate from the test dataset [10], [11]. The study results also showed that the CNN model might be the best AI model to detect cerebrovascular disease.

### **6.3 Recommendations**

- I. Many aspects such as network architecture, activation functions, regularization mechanisms, and optimization techniques, among other CNN related topics, have

all been improved. The rigorous demand that CNNs receives images of the same size has not, however, received much attention. In other words, CNN detection requires that all images be resized to a given size. This study resized the images to equal size. Our future work focuses on finding other alternatives ways to fed CNN model images of different sizes even if it means that CNN be reformed.

- II. The training procedure could be improved by using a larger MRI dataset. These techniques could also be used to solve other, more challenging, and clinically significant medical imaging issues that require research.

#### **6.4 Conclusion**

The study aim was to implement the CNN model for detection of cerebrovascular disease. The CNN model was trained using the images with cerebrovascular disease and images without cerebrovascular disease so that the model can tell if the image presented has cerebrovascular disease or not. Our study showed that the CNN model can successfully detected cerebrovascular disease with high validation accuracy rate of 90% and test accuracy rate of 80%.

## REFERENCES

- [1] World Health Organization. Global status report on non-communicable diseases 2014. Geneva: WHO.
- [2] Mortality and causes of death in South Africa, 2014: Findings from death notification / Statistics South Africa. Pretoria: Statistics South Africa.
- [3] Feigin, V.L., Lawes, C.M.M., Bennett, D.A., Barker-Collo, S.L., & Parag, V., 2014. Worldwide stroke incidence and early case fatality reported in 56 population-based studies: a systematic review. *Lancet Neurol.* Apr;8(4), pp. 355-369.
- [4] Sayed, E., 2014. Computer-aided Diagnosis of Human Brain Tumour through MRI: A Survey and a new algorithm, *Expert System with Applications*, pp.5526-5545.
- [5] Torteron, A.N.A., 2014. Consequences of false-positive screening mammograms. *JAMA Intern. Med.* 174, pp. 954–961.
- [6] Pouya, D.B., 2018. heart disease diagnosis using image processing by cuckoo algorithm before surgery. *Research in Medical and Engineering Science*, ISSN 2576-8816, pp. 250-252.
- [7] Jayashree, H., Alshwarya, B., Harsha, C., & Nisha, K., 2019. Skin disease detection using image processing with data mining and deep learning. *International Journal of Engineering Research and Technology (IJERT)*, Vol:06, Issue:04, pp. 4363-4366.

- [8] Shrikant, P., & Nisha, V.M., 2019. Early detection of alzheimers disease using image processing. International Journal of Engineering Research and Technology (IJERT), Vol:08, Issue:05, pp.468-471.
- [9] Abdulrahman, A., 2015. Segmentation of brain stroke image. International Journal of Advanced Research in Computer and Communication Engineering (IJARCCE), Vol:4, Issue: 9, pp. 375-378.
- [10] Sammy, V., & Brandon, G., 2020. Pneumonia detection using convolutional neural networks. International Journal of Scientific and Technology Research (IJSTR), Vol: 9, Issue: 4, pp. 1332-1337.
- [11] Žejmo, M., 2017. Classification of breast cancer cytological specimen using convolutional neural network. Journal of Physics: Conference Series. Vol: 783. No. 1. IOP Publishing, 2017, pp.1-11.
- [12] Masum, S.J., Abus, N.S., Nipa, A., Baharl, I., & Afsana, A.J., 2020. EczemaNet: A deep CNN-based eczema diseases classification. International Conference on Image Processing, Application and Systems (IPAS), December 2020, pp.174-179.
- [13] Tharani, S., & Yamini, C.,2016. Classification using convolutional neural network for heart and diabetics datasets. International Journal of Advanced Research in Computer and Communication Engineering (IJARCCE),Vol: 5, Issue: 12, pp. 417-422.
- [14] Geeth, M., Radhika, P., Priya, S., & Latha, S.R., 2021. Cerebrovascular accident prediction using logistic regression algorithm. International Journal of Engineering Research and Technology (IJERT), Vol: 8, Issue: 7, pp. 220-224.
- [15] Poovarasana, B., Sudherson, M., Sundarakrishnam, D., & Sureshkumar, S., 2019. Robotic arm for cerebrovascular accident patient by using Wi-Fi module. International

Journal of Innovative Research in advanced Engineering (IJIRAE), Vol: 6, Issue 3, pp. 138-142.

[16] Benuzillo, J., Savitz A., & Evans, S., 2019. Improving health care with advanced analytics: practical considerations. The Journal for Electronic Health Data and Methods (JEHDM), Vol: 3, Issue: 7, pp. 1-3.

[17] Zhao, X., Wu, Y., Song, G., Li, Z., Zhang, Y., & Fan, Y., 2018. A deep learning model integrating FCNNs and CRFs for brain tumour segmentation. Med. Image Anal. 43, pp. 98–111.

[18] Shi, Y., & Wardlaw, J., 2016. Update on cerebral small vessel disease: a dynamic whole-brain disease. Stroke Vasc Neurol. Vol: 3, Issue: 1, pp. 83-92.

[19] Fassbender, K., Balucani, C., Walter, S., Levine, S. R., Haass, A., & Grotta, J. 2013. Streamlining of prehospital stroke management: The golden hour. The Lancet Neurology, 12(6), pp. 585-596.

[20] Leeflang, M.M.G., 2018. Annals of internal medicine academia and clinic. academia and clinic 149(12), pp. 889–898.

[21] Jalab, H., & Alwaeli, A.M., 2019. Magnetic resonance imaging segmentation techniques of brain tumors: A review. Archives of Neuroscience In Press (In Press), pp. 1–7.

[22] Kamnitsas, K., 2015. Multi-scale 3D convolutional neural networks for lesion segmentation in brain MRI. Ischemic stroke lesion segmentation 13, p.46.

[23] Maier, O., 2017. A public evaluation benchmark for ischemic stroke lesion segmentation from multispectral MRI. Medical Image Analysis 35, pp. 250–269.

- [24] Jin, L., 2014. A Survey of MRI-based brain tumor segmentation methods jin. Tsinghua Science and Technology .19 (6), pp. 578–595.
- [25] Kesavaraj, G. & Sukumaran, S., 2013. A study on classification techniques in data mining. Fourth International Conference on Computing, Communications and Networking Technologies (ICCCNT) .IEEE pp.1-7.
- [26] Juan-Albarracín, J., 2015. Automated glioblastoma segmentation based on a multiparametric structured unsupervised classification. Plos one 10(5), pp. 1–20.
- [27] Fink, J.R., 2015. Multimodality brain tumor imaging: MR imaging, PET, and PET/MR imaging. Journal of Nuclear Medicine, 56(10), pp.1554-1561.
- [28] Hu, X., 2020. Brain SegNet: 3D local refinement network for brain lesion segmentation. BMC Medical Imaging, 20(1), pp.1-10
- [29] Goetz, M., 2015. DALSA: Domain adaptation for supervised learning from sparsely annotated MR Images. IEEE Transactions on Medical Imaging 35(1), pp. 184–196.
- [30] Feng, C., 2015. Segmentation of ischemic stroke lesions in multi-spectral MR images using weighting suppressed FCM and three phase level set. Springer, Cham. pp. 233-245.
- [31] Hassan, E., & Aboshgifa, A., 2015. Detecting brain tumour from MR image using matlab GUI programme. International Journal of Computer Science & Engineering Survey 6(6), pp. 47–60.
- [32] Harefa, J., 2017. Comparison classifier: support vector machine (SVM) and Knearest neighbor (K-NN) in digital mammogram images. Jurnal Informatika dan Sistem Informasi, 2(2), pp.35-40.

- [33] Subbanna, N.K., 2019. Stroke lesion segmentation in FLAIR MRI datasets using customized markov random fields. *Frontiers in Neurology*, pp.1-10.
- [34] Barucci, A., Carpi,R., Esposito,M., Olmastroni, M., & Zatelli, G., 2016. Diffusion-Weighted MR imaging: Clinical applications of kurtosis analysis to prostate cancer. *IFAC-TSRR*, Vol. 8, pp.67-78.
- [35] Castillo, L.S., Daza, L.A.,Rivera, L.C., & Arbelaez, p., 2017. Volumetric multimodality neural network for brain tumor segmentation. In *13th International Conference on Medical Information Processing and Analysis* . International Society for Optics and Photonics, 10572E, pp. 1-8.
- [36] Fasihi, M. S. & Mikhael, W.B., 2016. Overview of current biomedical image segmentation methods. *2016 International Conference on Computational Science and Computational Intelligence* , pp. 803–808.
- [37] Lorenzo, P.R., 2019. Segmenting brain tumors from FLAIR MRI using fully convolutional neural networks. *Computer methods and programs in biomedicine*, 176, pp.135-148.
- [38] Chen, L., 2018. Apparent diffusion coefficient value for prediction of hemorrhagic transformation in acute ischemic infarction. *11(1)*, pp. 109–117.
- [39] Gordillo, N., 2013. State of the art survey on MRI brain tumor segmentation. *31*, pp. 1426–1438.
- [40] Casamitjana, A., 2017. Cascaded V-Net using ROI masks for brain tumor segmentation. In *International MICCAI Brainlesion Workshop* .Springer, Cham. pp. 381-391.



- [41] Badrinarayanan, V., Kendall, A., & Cipolla, R., 2017. Segnet: A deep convolutional encoder-decoder architecture for image segmentation. *IEEE Transactions on Pattern Analysis and Machine Intelligence* 39(12), pp.1-14.
- [42] Sachin, R. J., Shubham S.S., Harshal, S. M., Akhilesh D.R., & Nishant, G. L., 2020. Brain Tumor Detection using Convolutional Neural Network. *International Research Journal of Engineering and Technology (IRJET)*, Vol: 07, Issue 01, pp,1232-1236.
- [43] Kamnitsas, K., 2018. Ensembles of multiple models and architectures for robust brain tumour segmentation. In *International MICCAI Brainlesion Workshop*. Springer, Cham. pp. 450-462.
- [44] Bauer, S., 2013. Integrated segmentation of brain tumor images for radiotherapy and neurosurgery. *International Journal of Imaging Systems and Technology* 23(1), pp. 59–63.
- [45] Alvarez, J.M., 2012. Road scene segmentation from a single image. In *European Conference on Computer Vision*. Springer, Berlin, Heidelberg. pp. 376-389.
- [46] Bakas, S., 2017. Advancing the cancer genome atlas glioma MRI collections with expert segmentation labels and radiomic features. *Scientific Data* 4(July), pp. 1–13.
- [47] Chitradevi, A., & Sadasivam, V., 2016. Various approaches for medical image segmentation: A survey. *Current Medical Imaging Reviews* 12(2), pp. 77–94.
- [48] Azhari, E.E.M., Hatta, M.M., Htike, Z., & Win, S.L., 2014. Tumor detection in medical imaging: A survey. *International Journal of Advanced Information Technology*, 4(1), pp.21-29.
- [49] Patil, D.D., & Deore, S.G., 2013. Medical Image Segmentation: A review. *International Journal of Computer Science and Mobile Computing* 2(1), pp. 22–27.

- [50] Razzak, M.I., 2018. Efficient brain tumor segmentation with multiscale two pathway-group conventional neural networks. *IEEE Journal of Biomedical and Health Informatics*, 23(5), pp.1911-1919.
- [51] Kaur, E.N., & Kaur, E.Y. 2015. Object classification techniques using machine learning model. *International Journal of Computer Trends and Technology* 18(4), pp. 170–174.
- [52] Niyazi, M. 2016. ESTRO-ACROP guideline “target delineation glioblastomas”. *Radiation Therapy and Oncology*, 118(1), pp.35-42.
- [53] Noh, H., 2015. Learning deconvolution network for semantic segmentation. In: *Proceedings of the IEEE International Conference on Computer Vision.*, pp. 1520–1528.
- [54] Long, J., 2015. Fully convolutional networks for semantic segmentation. *IEEE Transactions on Pattern Analysis and Machine Intelligence* 39(4), pp. 640–651.
- [55] Odland, A., 2015. Volumetric glioma quantification : comparison of manual and semi-automatic tumor segmentation for the quantification of tumor growth. 56(11), pp. 1396–1403.
- [56] Ronneberger, O., 2015. U-net: Convolutional networks for biomedical image segmentation. In *International Conference on Medical Image Computing and Computer-Assisted Intervention* (pp. 234-241). Springer, Cham.
- [57] Amiri, S., 2016. Deep random forest-based learning transfer to SVM for brain tumor segmentation. In: *2nd International Conference on Advanced Technologies for Signal and Image Processing, ATSIP 2016.*, pp. 297–302.

- [58] Majnik, M., & Bosni, Z., 2013. ROC analysis of classifiers in machine learning: A survey. *Intelligent Data Analysis* 17(3), pp. 531–558.
- [59] Menze, B., 2015. The multimodal brain tumor image segmentation benchmark (BRATS). *IEEE Transactions on Medical Imaging* 34. pp:11-15
- [60] Li, J., 2017. Pedestrian detection with dilated convolution, region proposal network and boosted decision trees. *Proceedings of the International Joint Conference on Neural Networks 2017-May*, pp. 4052–4057.
- [61] Norouzi, A., 2014. Medical image segmentation methods, algorithms, and applications. *IETE Technical Review (Institution of Electronics and Telecommunication Engineers, India)* 31(3), pp. 199–213.
- [62] Prasanna, P., Karnawat, A., Ismail, M., Madabhushi, A., & Tiwari, P., 2019. Radiomics-based convolutional neural network for brain tumor segmentation on multiparametric magnetic resonance imaging. *Journal of Medical Imaging*, 6(2), pp.1-10.
- [63] Robben, D., 2015. A Voxel-wise, cascaded classification approach to ischemic stroke lesion segmentation. In *BrainLes 2015* pp. 254-265
- [64] Shelhamer, E., 2017. Fully convolutional networks for semantic segmentation. *IEEE Transactions on Pattern Analysis and Machine Intelligence* 39(4), pp. 640–651.
- [65] Farfade, S.S., Saberian, M.J., & LiL, J., 2015 Multi-view face detection using deep convolutional neural networks. In: *5th international conference on multimedia retrieval*. New York: ACM. pp. 643–50.
- [66] Goodfellow, I.J., Warde-Farley, D., Mirza, M., Courville, A., & Bengio, Y., 2013. Max-out networks. In: *Proceedings of the 30th international conference machine learning*. pp. 1319–27.

[67] He, K., Zhang, X., Ren, S., & Sun, J., 2015 Delving deep into rectifiers: surpassing human-level performance on image net classification. In: Proceedings of the IEEE international conference on computer vision. pp. 1026–34.

[68] Hashemi, M., & Hall. M., 2019. Detecting and classifying online dark visual propaganda. *Image Vis Compute*, 89(1):95–105.

[69] SALMA, A.R.,2020. Deep Learning-based Brain Tumour Image Segmentation and its Extension to Stroke Lesion Segmentation. *Cadiff University*.pp.39-170